

ORIGINAL RESEARCH

Profiling Daily Life Performance Recovery in the Early Subacute Phase After Stroke Using a Graphical Modeling Approach

Janne M. Veerbeek , PhD*; Clemens Hutter , MSc*; Beatrice Ottiger, MSc; Soel Micheletti , MSc; Simone Riedi , MSc; Enrico Bianchi , MSc; Noortje Maaijwee, MD; Tim Vanbellingen , PhD; Thomas Nyffeler , MD

BACKGROUND: Laboratory-based assessments have shown that stroke recovery is heterogeneous between patients and affected domains such as motor and language function. However, laboratory-based assessments are not ecologically valid and do not necessarily reflect patients' daily life performance. Therefore, we aimed to give an innovative view on stroke recovery by profiling daily life performance recovery across domains in patients with early subacute stroke and determine their interrelatedness, taking stroke localization into account.

METHODS AND RESULTS: Daily life performance was observed at neurorehabilitation admission and weekly thereafter until discharge, using a scale containing 7 daily life domains. Graphical modeling was applied to investigate the conditional independence between recovery of these domains depending on stroke localization. There were 592 patients analyzed. Four clusters of interrelated domains were identified within the first 6 weeks poststroke. The first cluster included recovery in learning and applying knowledge, general tasks and demands, and domestic life. The second cluster comprised recovery in self-care and general tasks and demands. The third cluster included recovery in mobility and self-care; it incorporated interpersonal interactions and relationships in left supratentorial stroke, and learning and applying knowledge in right supratentorial stroke. The final cluster included only communication recovery.

CONCLUSIONS: Daily life recovery dynamics early poststroke show that although impairments in body functions are anatomically determined, their impact on performance is comparable. Second, some, but by no means all, domains show an interrelated recovery. Domains requiring cognitive abilities are especially interrelated and seem to be essential for concomitant recovery in mobility and domestic life.

Key Words: stroke ■ recovery ■ prognosis ■ activities and participation ■ performance ■ conditional independence ■ graphical modeling

Stroke recovery is complex and not fully unraveled to date. However, there is general agreement that recovery predominantly takes place within the first 3 to 6 months poststroke, with most changes occurring within the first weeks to months.¹ This pattern has been observed for different domains including motor function,² somatosensory function,³ speech,⁴ and cognition.⁵ Moreover, it has also been shown that recovery is

variable within and between domains, and that recovery of 1 domain can be mediated by others. For instance, patients without visuospatial neglect improved their upper limb motor function better and quicker than those with visuospatial deficits.⁶

To capture the pattern and heterogeneity of stroke recovery across domains, Ramsey and colleagues grouped body functions in the motor, language,

Correspondence to: Janne M. Veerbeek, PhD, Neurocenter, Luzerner Kantonsspital, Spitalstrasse, 6000 Lucerne, Switzerland. Email: janne.veerbeek@luks.ch

*J. M. Veerbeek and C. Hutter are co-first authors.

This article was sent to Kori S. Zachrison, MD, MSc, Associate Editor, for review by expert referees, editorial decision, and final disposition.

Supplemental Material is available at <https://www.ahajournals.org/doi/suppl/10.1161/JAHA.123.030472>

For Sources of Funding and Disclosures, see page 10.

© 2023 The Authors. Published on behalf of the American Heart Association, Inc., by Wiley. This is an open access article under the terms of the [Creative Commons Attribution-NonCommercial-NoDerivs](https://creativecommons.org/licenses/by-nc-nd/4.0/) License, which permits use and distribution in any medium, provided the original work is properly cited, the use is non-commercial and no modifications or adaptations are made.

JAHA is available at: www.ahajournals.org/journal/jaha

CLINICAL PERSPECTIVE

What Is New?

- Daily life performance recovery across domains early after stroke is heterogeneous, and even if impairments in body functions are determined anatomically, they have a similar impact on daily life performance (recovery).

What Are the Clinical Implications?

- The results highlight the importance of evaluating daily life performance of patients with stroke in addition to laboratory-based tests for single domains such as motor, cognitive, or speech function.
- The present study provides the groundwork for future patient-specific, dynamic prediction models (including factors such as age, sex, and comorbidities) for various daily life performance domains that may improve poststroke care and positively impact patients' daily life performance.

Nonstandard Abbreviations and Acronyms

ICF	<i>International Classification of Functioning, Disability, and Health</i>
------------	--

memory, and attention domains at around 2 weeks, as well as 3 and 12 months poststroke.⁷ Early after stroke, they detected 2 clusters of highly interrelated domains; the first cluster was made up of language, verbal memory, and spatial memory, whereas the second cluster was composed of motor function, attention, and spatial memory. The strength of the relations within the second cluster remained stable at 3 and 12 months, but disappeared within the first cluster. Furthermore, the degree of recovery as assessed by a ratio index did not show statistically significant differences between domains. However, the longitudinal relationship between domains was not described.

This previous work⁷ on across-domain recovery applied laboratory-based assessments measuring the patient's capacity in a uniform standard environment.⁸ However, these assessments may not necessarily reflect the patient's performance in daily life,⁹ because there are more demands on functioning in real life than there are for executing a task in a controlled laboratory setting without distraction. In this context, performance is defined as what an individual does in his or her current environment⁸ according to the *International Classification of Functioning, Disability, and Health (ICF)*. The questionable ecological validity

of laboratory-based tests was also recently demonstrated for recovery on the motor domain.⁹ Real-world arm use in patients with stroke as assessed by accelerometers already plateaued 3 to 6 weeks poststroke, although further improvements on laboratory-based upper limb motor assessments beyond this time-frame were observed.⁹ These findings underline the importance of investigating what patients do in daily life across multiple time points and domains. Although currently lacking, this information is essential for improving our understanding of stroke recovery, and impacts on rehabilitation program design. The *ICF* framework,⁸ with its Activities and Participation component, is well suited to capture the patient's daily life performance as the patient's execution of a task or action⁸ and involvement in a life situation⁸ are observed. It has been shown that applying this *ICF* framework provides a more extensive overview of the patient's functioning than laboratory-based assessments alone.¹⁰ When investigating daily life performance recovery following stroke, the sample should not only be analyzed as a whole, but also stratified according to stroke localization. Although body functions are anatomically determined,¹¹ long-term overall outcome as assessed with the modified Rankin Scale is comparable.¹² It is unclear whether differences in terms of daily life performance (recovery) across multiple domains exist. Through graphical modeling, dependencies between domains can be visualized by an interpretable graph (network), facilitating the intuitive understanding of potentially complex data.¹³ Such an approach has seen increasing in popularity in the past decade in clinical neurology research, and it has been found to be clinically meaningful.^{13–15}

The main aims of this study were to determine in a large sample of patients with early subacute stroke during inpatient rehabilitation whether (1) differences in performance across 7 domains from the Activities and Participation component of the *ICF* exist, depending on the stroke localization, and (2) the longitudinal recovery profiles of these domains are interrelated in the whole sample as well as in stroke localization subgroups, based on weekly repeated measurements. Weekly repeated measurements were chosen because it is unknown what the recovery dynamics of early poststroke recovery on daily life performance look like, and whether they match observations from laboratory-based assessments that most changes take place early after stroke.¹

METHODS

Data and Code Disclosure Statement

Because the study participants did not sign an agreement that allows the open sharing of the acquired data,

the conditions of our ethics approval do not permit public archiving of the data supporting the conclusions of this study. Based on the Swiss Human Research Act (Humanforschungsgesetz) in Switzerland, readers seeking access to the data and the study materials must complete a formal data sharing agreement to obtain the data. Interested readers should contact the corresponding author (J.M.V.) for more information and help. All deidentified data that are necessary and sufficient to replicate all data processing steps and analyses will be shared with requestors who meet these requirements.

All analyses were performed in Python, and the code is publicly available at [<https://github.com/rauwcckl/CorrelationGraph4StrokeRecovery>].

Patients

This is a retrospective analysis of data routinely collected in patients with early subacute stroke admitted to the Neurocenter of the Luzerner Kantonsspital (Lucerne, Switzerland) for inpatient rehabilitation between January 2016 and March 2021. Patients ≥18 years of age who had suffered either an acute ischemic or hemorrhagic stroke (defined according to the European Stroke Organization guidelines) were included in the analysis if they (1) had entered rehabilitation ≤21 days after symptom onset and (2) had repeated measures of daily life performance observations during rehabilitation (see Assessment of Daily Life Performance Across Domains section) between every 5 to 10 days. The design of this longitudinal observational study is displayed in Figure 1. Details on rehabilitation content is described in Data S1.

Statistical Analysis

Assessment of Daily Life Performance Across Domains

Daily life performance during inpatient rehabilitation was assessed on the level of the Activities and Participation component of the ICF. For this purpose, the Lucerne ICF-based Multidisciplinary Observation Scale was applied, which is reliable, valid, and responsive.^{16,17} The Lucerne ICF-Based Multidisciplinary Observation Scale consists of 45 ICF items⁸ divided into 7 domains: (1) interpersonal interactions and relationships, (2) mobility, (3) self-care, (4) communication, (5) learning and applying knowledge, (6) tasks and demands, and (7) domestic life. The definitions of these domains are provided in Table S1. Each item is rated on a 5-point Likert scale, ranging from 1 (patient is not able to fulfill a task or needs assistance of <75% [ie, complete assistance]) to 5 (patient is able to fulfill task independently [ie, no assistance needed]) (Table S2). All Lucerne ICF-Based Multidisciplinary Observation Scale items were rated by trained members of the multidisciplinary team at rehabilitation admission on a weekly basis during the rehabilitation stay, and at discharge. Thus, we obtained a sequence (or time series) of measurements.

Cross-Sectional Analysis of Daily Life Performance at Rehabilitation Admission

The items making up each ICF domain were averaged per patient and measurement time point, whereas missing values in individual items were ignored. If all items of a domain were missing, then the corresponding measurement was excluded. Subsequently, the values at rehabilitation admission were compared for

Downloaded from <http://ahajournals.org> by on August 16, 2023

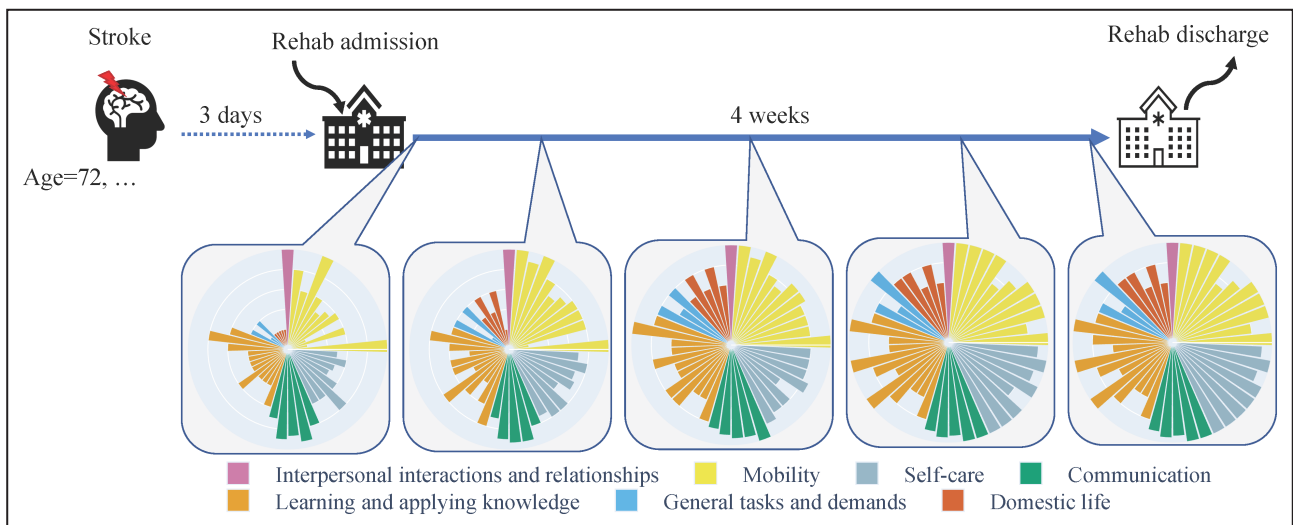


Figure 1. Study design based on 1 exemplary patient.

The colors represent 7 daily life domains from the Activities and Participation component of the *International Classification of Functioning, Disability, and Health*.

each domain between stroke localization regions (supratentorial left, supratentorial right, infratentorial) using the nonparametric Kruskal-Wallis H test. When this test was statistically significant for a domain, a post hoc pairwise comparison was performed using the Dunn test.¹⁸ Throughout, we use the Bonferroni correction to adjust significance levels for multiple comparisons.

Graphical Modeling

We model the relationships between weekly recovery in 7 ICF domains during inpatient neurorehabilitation using an undirected graph. Nodes (circles) correspond to domains, whereas edges (lines) describe their relationships when accounting for all other domains. Because we are interested in patients' recovery profiles over time, we rely on the particularly suitable method introduced by Dahlhaus¹⁹ for time series data. Here we focus on the model interpretation, and refer to Sections A.2 and A.3 in Data S1 for a self-contained derivation of the methodology.

For each patient, we obtained a time series of 7 dimensional vectors, where each entry represents the average scores in the corresponding domain over time. We analyzed the score differences between consecutive weeks. To model this mathematically, we treated each time series as a realization of a common 7-dimensional stochastic process, which we assumed to be wide sense stationary and nondegenerate (Data S1).

We were interested in predicting the evolution of 2 domains $a, b \in \{1, \dots, 7\}$ from the past, present, and future values of all 5 remaining domains $R := \{1, \dots, 7\} \setminus \{a, b\}$ (Data S1). Then we considered whether the prediction error for the a -th domain is correlated with the prediction error for the b -th domain. If the errors were uncorrelated, then we considered the domains a and b to be unrelated, after accounting for the remaining domains (which we wrote as $a \perp b \mid R$, Data S1). This means that no additional information about the evolution of domain a can be obtained from

observing domain b once we have knowledge of the remaining domains R . This notion allows us to define the so-called partial correlation graph (Data S1), where 2 nodes a, b are not connected if they are unrelated in the above-mentioned sense (ie, if $a \perp b \mid R$ holds). Conversely, a, b are connected by an edge if the prediction errors are correlated. In addition, we visualized the strength of the relationship between 2 nodes by varying the edge thickness; the thicker the edge, the stronger the correlation of the prediction errors. We identified a drop in this relationship strength after the sixth edge (Data S1), and thus visualized the 6 strongest edges in the graphs.

Bootstrapping was used to assess the robustness of the procedure. We repeated the analysis 10 000 times, each time using a new bootstrap replicate of the data set and counted how often the obtained edges differed.

Ethics and Reporting Guideline

All analyzed patients provided their general consent in written form. Analyses of the data were approved by Cantonal Ethics Committee Northwest and Central Switzerland (BASEC-ID 2017-00998). Reporting adhered to the Strengthening the Reporting of Observational Studies in Epidemiology statement.²⁰

RESULTS

Patients

Data of 592 patients with early subacute stroke were analyzed (see Figure 2 for the flowchart). Patients' characteristics are described in Table 1, and exemplary recovery profiles are provided in Figure 3.

Cross-Sectional Analysis of Daily Life Performance Data at Admission

Comparing the ICF domain scores at rehabilitation admission between stroke localization regions showed overall statistically significant differences for all domains

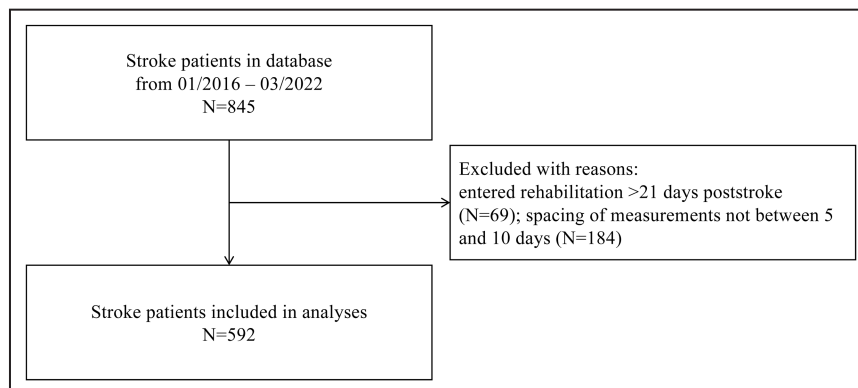


Figure 2. Data selection flowchart.

Table 1. Patients' Characteristics

Characteristic	Value (N=592)	Missing values (%)
Age, y, mean (SD)	71.7 (14.4)	0
Sex, women, n (%)	267 (45.1)	0
Time poststroke, d, median (q1–q3)	8.0 (6.0–10.0)	0
Length of stay, d, median (q1–q3)	28.0 (19.0–40.0)	0
NIHSS, /42, median (q1–q3)*	4.0 (2.0–8.0)	12.5
Stroke localization, n (%)		0
Supratentorial left	274 (46.3)	
Supratentorial right	198 (33.4)	
Infratentorial	120 (20.3)	
LIMOS at admission, median (q1–q3)		0
Total score, /35	21.0 (16.2–25.8)	
Interpersonal interactions and relationships, /5	4.0 (3.0–4.0)	
Mobility, /5	3.1 (2.3–3.8)	
Self-care, /5	3.4 (2.4–4.1)	
Communication, /5	3.6 (2.5–4.5)	
Learning and applying knowledge, /5	2.9 (2.2–3.7)	
General tasks and demands, /5	2.3 (1.7–3.0)	
Domestic life, /5	2.0 (1.2–2.8)	

ICF indicates *International Classification of Functioning, Disability, and Health*; LIMOS, Lucerne ICF-based Multidisciplinary Observation Scale; NIHSS, National Institutes of Health Stroke Scale; and q1–q3, quartile 1 to quartile 3.

*In case of thrombolysis and thrombectomy, the value refers to the first NIHSS assessment after acute treatment.

(Table 2, Figure 4). The post hoc comparisons between regions are shown in Table 2.

Graphical Modeling

The results of the graphical modeling are depicted in Figure 5. Out of 21 domain pairs, 6 pairs were found to be strongly interrelated during rehabilitation in the early subacute phase poststroke. Grouping interrelated domains resulted in 4 clusters. The first cluster included recovery in learning and applying knowledge, general tasks and demands, and domestic life. The second cluster was built by recovery in self-care and general tasks and demands. The third cluster consisted of recovery in mobility, self-care, and interpersonal interactions and relationships. The final cluster focused only on communication recovery. The bootstrapping procedure showed a good robustness except for the relationship between interpersonal interactions and relationships and self-care, which was missing in 24.5% of the bootstrap samples (Table S3).

Repeating the graphical modeling approach in the supratentorial left subgroup showed a similar picture (Figure 6A). In supratentorial right strokes' third cluster, an additional relationship was found between mobility and learning and applying knowledge, whereas

no relationship existed between self-care and interpersonal interactions and relationships (Figure 6B). A graph could not be constructed for infratentorial strokes, because the sample size was too small.

DISCUSSION

We presented an innovative view on stroke recovery by analyzing daily life performance from a multidomain perspective in a heterogeneous sample of 592 patients with early subacute stroke. The cross-sectional analysis of data collected 1 week poststroke showed that the patients' daily life performance during rehabilitation in the domains general tasks and demands, and domestic life was clearly lower than in the other 5 domains. One explanation for this could be that within these 2 domains, the patients' performance in complex daily life activities was observed, requiring high levels of functioning on the motor, cognitive, and communicative domains, as well as a good integration thereof.²¹ Patients with infratentorial stroke had a significantly higher performance on all domains (except for mobility), when compared with those who suffered a supratentorial stroke. The finding that only mobility performance was equal between infra- and supratentorial strokes might be a result of the differences in symptoms. Although the cerebellum²² and brainstem²³ also play a role in cognition, cognitive deficits are less common in infratentorial strokes than in supratentorial strokes.²⁴ Comparing patients with left supratentorial stroke with right supratentorial stroke showed only significant differences in the mobility and communication domains. Lower mobility performance was seen in patients with right supratentorial stroke, which may be related to the presence of unilateral spatial neglect in these patients.²⁵ It has been shown that patients with neglect have more limitations in posture and movement,²⁶ and upper limb motor function²⁷ when compared with those without neglect. Conversely, patients with left supratentorial stroke showed a lower communication performance, which is in line with the well-known lateralization of language in the left hemisphere.²⁸

In a further step, we analyzed the longitudinal relationship between recovery during the first 6 weeks poststroke in the 7 daily life domains during rehabilitation in the whole sample using a graphical modeling approach. Among 21 possible domain pairs, 6 were strongly interrelated. These pairs were identical to the domain pairs when only supratentorial left strokes were considered. In right supratentorial strokes, 5 of these 6 relationships were identical, and 1 was different. This suggests 2 things: first, that recovery across domains is heterogeneous, and second, that although impairments in body functions are determined anatomically,

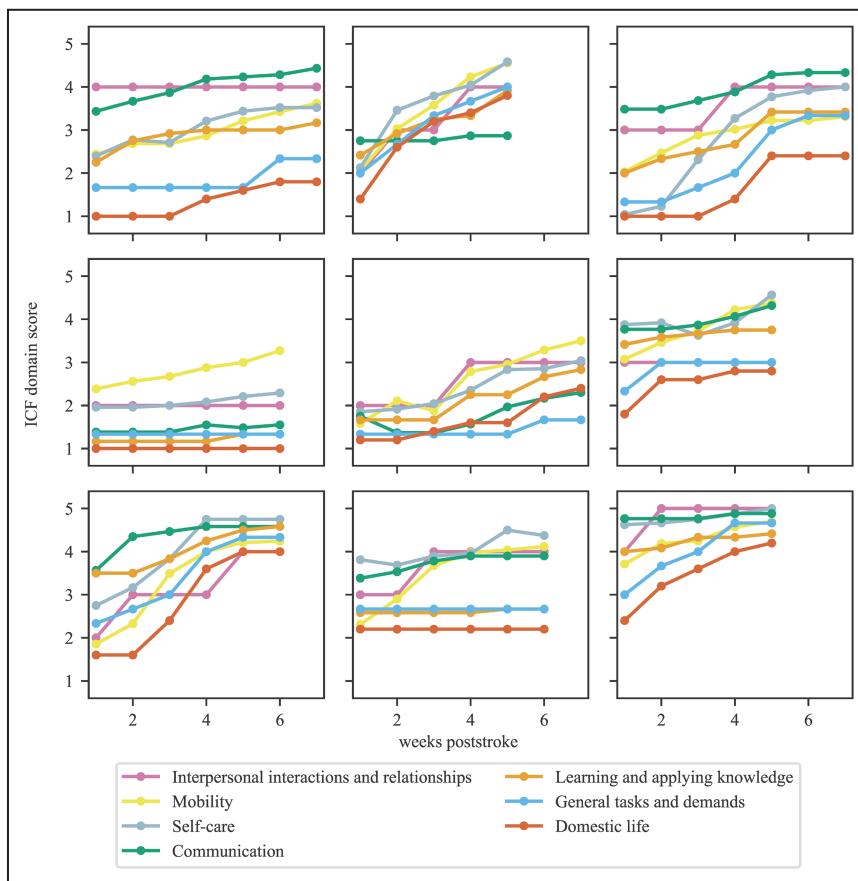


Figure 3. Examples of recovery profiles of 9 early subacute patients for 7 daily life domains from the Activities and Participation component of the ICF. ICF indicates International Classification of Functioning, Disability, and Health.

they have a similar impact on daily life recovery during inpatient rehabilitation. From the graphical modeling, a total of 4 clusters (ie, groups of interrelated domains) for daily life performance recovery could be observed. First, a strong interrelatedness was found between learning and applying knowledge, general tasks and

demands, and domestic life. This observation was also found when the left and right supratentorial strokes were analyzed separately. The ability to manage complex everyday life requires a good integration of higher-level cognitive and motor performance, which could be one explanation.²⁹ We speculate that recovery of

Table 2. Comparison of Daily Life Domain Scores at Rehabilitation Admission From the Activities and Participation Component of the ICF Between Stroke Localizations

ICF domain	Kruskal-Wallis H test, P value	Post hoc analysis, P value		
		Supratentorial left vs supratentorial right	Supratentorial left vs infratentorial	Supratentorial right vs infratentorial
Interpersonal interactions and relationships	<0.001*	0.073	<0.001*	0.037
Mobility	0.004*	<0.001*	0.456	0.048
Self-care	<0.001*	0.008	0.072	<0.001*
Communication	<0.001*	<0.001*	<0.001*	0.002*
Learning and applying knowledge	<0.001*	0.929	<0.001*	<0.001*
General tasks and demands	<0.001*	0.095	<0.001*	<0.001*
Domestic life	<0.001*	0.025	0.009	<0.001*

ICF indicates International Classification of Functioning, Disability, and Health. *P values are significant at P<0.05 after Bonferroni correction for multiple comparisons.

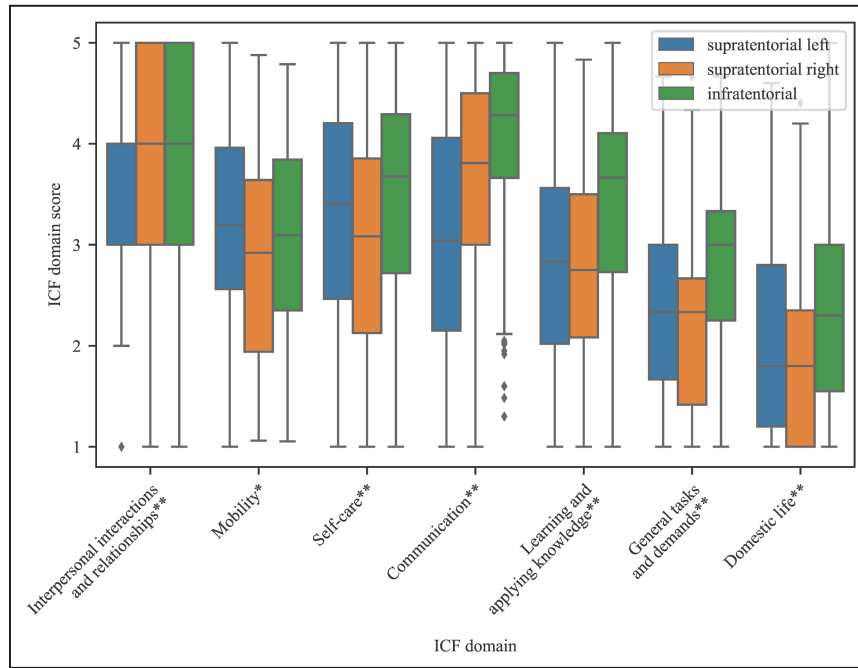


Figure 4. Daily life domain scores at rehabilitation admission from the Activities and Participation component of the ICF by stroke localization. ICF indicates *International Classification of Functioning, Disability, and Health*. * $P < 0.05$ after Bonferroni correction for multiple comparisons; ** $P < 0.01$ after Bonferroni correction for multiple comparisons.

cognition drives recovery of everyday life, and that cognitive–motor interference results in a deterioration of daily life performance.³⁰

The second cluster of interrelated domains consists of recovery in self-care and general tasks and demands. For both domains, cognitive and motor recovery seem to be equally important. Taking dressing as an example item that is contained in the self-care domain, we see a task in which patients must select appropriate clothing, determine the right order, and should be physically able to perform relevant motor acts and apply compensation strategies, if needed. From isolated observations, we know that paresis, apraxia, and neglect are the main drivers for dressing limitations.³¹ In the same vein, observed general tasks and demands tasks, such as making a bed, managing diabetes, and making payments online, rely on both cognitive and motor functions. They distinguish themselves from self-care items by their less-routine nature (ie, these tasks belong to instrumental activities of daily living).

The third cluster includes recovery in mobility and self-care. In left supratentorial strokes, interpersonal interactions and relationships recovery was also included. In patients with right supratentorial stroke, this cluster also contained learning and applying knowledge recovery, although this latter relationship was weaker than the other 5 found relationships. The

mobility–self-care relationship could be explained by the fact that mobility activities are often also used during self-care. For example, when recovery in the mobility-item hand and arm use (ICF code d445) is present, recovery in the self-care item washing oneself (ICF code d510) will most likely be observed in parallel, because recovery in hand and arm use is required to improve on these items. In addition, both domains might be largely influenced by the presence of a paresis and neglect.^{6,32} The lack of an overall relationship between mobility recovery and the more nonmotor ICF domains could be related to the strong dependency of mobility recovery on corticospinal tract integrity,^{7,33} whereas cognition is more dependent on an intact function of widespread (sub)cortical networks.³⁴ However, a relationship between mobility and learning and applying knowledge was present in right supratentorial strokes. In both domains, the presence of right hemispheric symptoms like neglect and anosognosia may have a detrimental effect on performance.^{32,35} This longitudinal relationship matches the cross-sectional relationship between motor function and attention observed by Ramsey and colleagues.⁷ The presence of aphasia may be the reason why interpersonal interactions and relationships were included in this third cluster in supratentorial left strokes, because previous work has shown that aphasia negatively influences interpersonal relationships³⁶ and hampers care provision.³⁷

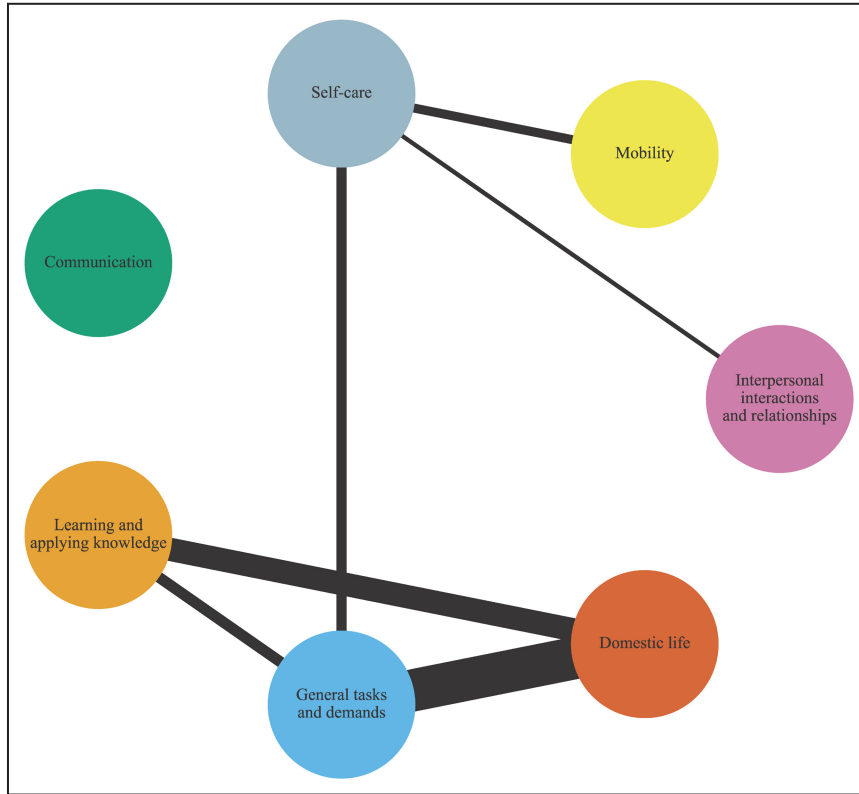


Figure 5. Partial correlation graph for the entire sample (N=592). Each node (circle) represents a daily life domain from the Activities and Participation component of the *International Classification of Functioning, Disability, and Health*. Each edge (line) represents a direct relationship between recovery of 2 domains that persists when accounting for all other 5 domains.

The fourth and final cluster includes recovery of communication performance, which was unrelated to recovery in the other 6 domains. This finding was

shown for the entire sample, as well as in patients with supratentorial left stroke, in which aphasia is more often present.⁴ Data inspection showed generally

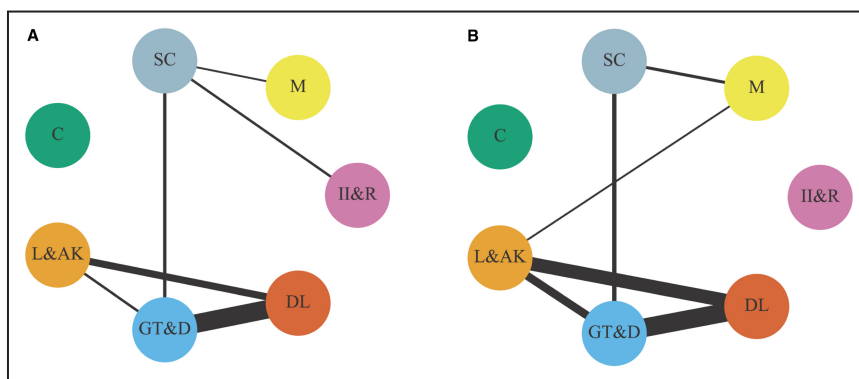


Figure 6. Partial correlation graphs for left (N=274) and right supratentorial strokes (N=198). Each node (circle) represents a daily life domain from the Activities and Participation component of the *International Classification of Functioning, Disability, and Health*. Each edge (line) represents a direct relationship between recovery of 2 domains that persists when accounting for all other 5 domains. **A**, patients with left supratentorial stroke. **B**, Patients with right supratentorial stroke. C indicates communication; DL, domestic life; GT&D, general tasks and demands; II&R, interpersonal interactions and relationships; L&AK, learning and applying knowledge; M, mobility; and SC, self-care.

Downloaded from <http://ahajournals.org> by on August 16, 2023

less recovery on the communication domain in daily life during the first 2 months poststroke in inpatient rehabilitation. This result agrees with findings from laboratory-based tests. For instance, Dunn and colleagues showed that in the acute phase poststroke, the recovery curve of language was less steep when compared with motor recovery.³⁸

Surprisingly, the graphical modeling approach barely displayed differences between patients with left and right supratentorial stroke. This suggests that although symptoms between strokes in the left and right hemisphere vary on a Body Function component (eg, aphasia in left hemispheric strokes, neglect occurs more often in right hemispheric strokes),³⁹ the interrelatedness between recovery on various performance domains, or the lack thereof, is equal. From this observation, the anatomical lateralization of functions seems to be less relevant when looking at recovery of daily life performance during inpatient rehabilitation. However, from a treatment perspective, it is likely that different approaches are required to enhance daily life performance recovery in each of these subgroups. The cross-sectional analysis also points toward a possible impact of stroke symptoms such as a hemiparesis, neglect, and aphasia on daily life performance, although they might impact in a different manner. Especially higher-order domains such as general tasks and demands and domestic life, require a good integration of both motor and nonmotor functions and abilities. However, in the current work, we were unable to investigate possible associations with limitations on the body function component and recovery thereof. Thus, from a clinical perspective, knowledge of impairments of the Body Function component as well as limitations of the Activities and Participation component are important for adapting rehabilitation programs to the patient's individual needs.

Another relevant aspect of this work is related to cost-effectiveness. Increasing health care costs force us to critically review the indication to continue rehabilitation in individuals constantly. The weekly observation of the patients' daily life performance is a critical aspect herein. This study shows that just focusing on laboratory-based testing of, for example, muscle strength to capture a paresis or visuospatial attention to assess neglect to determine whether to stop, continue, or adapt rehabilitation is too shortsighted. Although our sample had a median acute National Institutes of Health Stroke Scale of 4 (quartile 1=2, quartile 3=8) after thrombolysis and thrombectomy, we could show that although patients have mild-to-moderate deficits when using a quick bedside test on the Body Function component, they can have substantial restrictions in daily life performance.²⁹ Furthermore, it shows that the National Institutes of Health Stroke Scale does not

capture cognitive deficits sufficiently,⁴⁰ although cognition seems to play a central role in daily life performance during inpatient rehabilitation and its recovery.

Our analysis methodology comes with some caveats. Although we do not make any assumptions about the distribution of the data, we do assume the underlying stochastic process to be stationary. Furthermore, linear predictors are used, and we did not investigate the causality of relationships. Lastly, we determined the number of strong relationships to be 6, based on a drop in the strength of relationships, which comes with some ambiguity. On the clinical side, it is important to note that the observations were restricted to the first 2 months poststroke during inpatient neurorehabilitation. Our results cannot be generalized to the general stroke population, including patients with both less and more severe poststroke deficits who do not receive inpatient neurorehabilitation, and does not inform us about the chronic phase after stroke.

To improve generalizability of our results, future studies should include all patients with stroke regardless of stroke severity, and follow-up should be extended into the chronic phase. This would enable the inclusion of social and environmental modifiers of daily life performance recovery outside of an inpatient rehabilitation setting. Furthermore, our study is the groundwork for future studies on the relationship between recovery of body functions and daily life performance, as well as on the predictability of recovery of multiple real-life performance domains in individual patients. Clinical trials are needed to evaluate if rehabilitation interventions positively affect performance in interrelated domains. These could be informed by graphical modeling.¹³

CONCLUSIONS

To the best of our knowledge, this is the first study that investigated the impact of stroke localization on daily life performance during inpatient rehabilitation and the interrelatedness of weekly recovery on multiple daily life performance domains in patients with early subacute stroke based on a graphical modeling approach using time series. Independent of stroke localization, 4 clusters of interrelated performance domains were identified. This finding supports the use of scales that capture the patient's performance in daily life along with laboratory-based assessments. This will help health care professionals to timely identify restrictions that require further rehabilitative treatment, with the potential of developing better and more cost-efficient neurorehabilitation programs. This study sheds light on patients' recovery processes using daily life performance observations, therewith reinforcing the importance of managing everyday life and its demanding nature.

ARTICLE INFORMATION

Received April 6, 2023; accepted June 9, 2023.

Affiliations

Neurocenter, Luzerner Kantonsspital, Lucerne, Switzerland (J.M.V., B.O., N.M., T.V., T.N.); Chair for Mathematical Information Science (C.H.) and Department of Computer Science (S.M., S.R., E.B.), ETH Zurich, Zurich, Switzerland; ARTORG Center for Biomedical Engineering Research, Gerontechnology and Rehabilitation Group, University Bern, Bern, Switzerland (T.V., T.N.); and Department of Neurology, Inselspital, Bern University Hospital, University of Bern, Switzerland (T.N.).

Sources of Funding

This study was supported by the Swiss National Science Foundation (grant number 32003B_196915). The funder played no role in the research.

Disclosures

None.

Supplemental Material

Data S1

Tables S1–S3

Figures S1–S3

References^{41–44}

REFERENCES

- Bernhardt J, Hayward KS, Kwakkel G, Ward NS, Wolf SL, Borschmann K, Krakauer JW, Boyd LA, Carmichael ST, Corbett D, et al. Agreed definitions and a shared vision for new standards in stroke recovery research: the Stroke Recovery and Rehabilitation Roundtable Taskforce. *Neurorehabil Neural Repair*. 2017;31:793–799. doi: 10.1177/1545968317732668
- Duncan PW, Goldstein LB, Matchar D, Divine GW, Feussner J. Measurement of motor recovery after stroke. Outcome assessment and sample size requirements. *Stroke*. 1992;23:1084–1089. doi: 10.1161/01.str.23.8.1084
- Kessner SS, Schlemm E, Cheng B, Bingel U, Fiehler J, Gerloff C, Thomalla G. Somatosensory deficits after ischemic stroke. *Stroke*. 2019;50:1116–1123. doi: 10.1161/strokeaha.118.023750
- Pedersen PM, Jørgensen HS, Nakayama H, Raaschou HO, Olsen TS. Aphasia in acute stroke: incidence, determinants, and recovery. *Ann Neurol*. 1995;38:659–666. doi: 10.1002/ana.410380416
- Patel M, Coshall C, Rudd AG, Wolfe CD. Natural history of cognitive impairment after stroke and factors associated with its recovery. *Clin Rehabil*. 2003;17:158–166. doi: 10.1191/0269215503cr596oa
- Nijboer TC, Kollen BJ, Kwakkel G. The impact of recovery of visuo-spatial neglect on motor recovery of the upper paretic limb after stroke. *PLoS One*. 2014;9:e0100584. doi: 10.1371/journal.pone.0100584
- Ramsey LE, Siegel JS, Lang CE, Strube M, Shulman GL, Corbetta M. Behavioural clusters and predictors of performance during recovery from stroke. *Nat Hum Behav*. 2017;1:38. doi: 10.1038/s41562-016-0038-8
- World Health Organization. *Towards a Common Language for Functioning, Disability and Health: ICF*. World Health Organization; 2002.
- Lang CE, Waddell KJ, Barth J, Holleran CL, Strube MJ, Bland MD. Upper limb performance in daily life approaches plateau around three to six weeks post-stroke. *Neurorehabil Neural Repair*. 2021;35:903–914. doi: 10.1177/15459683211041302
- Zhang T, Liu L, Xie R, Peng Y, Wang H, Chen Z, Wu S, Ni C, Zheng J, Li X, et al. Value of using the International Classification of Functioning, Disability, and Health for stroke rehabilitation assessment: a multicenter clinical study. *Medicine (Baltimore)*. 2018;97:e12802. doi: 10.1097/md.00000000000012802
- Gazzaniga MS. Principles of human brain organization derived from split-brain studies. *Neuron*. 1995;14:217–228. doi: 10.1016/0896-6273(95)90280-5
- Fink JN, Frampton CM, Lyden P, Lees KR. Does hemispheric lateralization influence functional and cardiovascular outcomes after stroke? An analysis of placebo-treated patients from prospective acute stroke trials. *Stroke*. 2008;39:3335–3340. doi: 10.1161/strokeaha.108.523365
- Kalisch M, Fellinghauer BA, Grill E, Maathuis MH, Mansmann U, Bühlmann P, Stucki G. Understanding human functioning using graphical models. *BMC Med Res Methodol*. 2010;10:14. doi: 10.1186/1471-2288-10-14
- Massa MS, Wang N, Bickerton WL, Demeyere N, Riddoch MJ, Humphreys GW. On the importance of cognitive profiling: a graphical modelling analysis of domain-specific and domain-general deficits after stroke. *Cortex*. 2015;71:190–204. doi: 10.1016/j.cortex.2015.06.006
- Strobl R, Stucki G, Grill E, Müller M, Mansmann U. Graphical models illustrated complex associations between variables describing human functioning. *J Clin Epidemiol*. 2009;62:922–933. doi: 10.1016/j.jclinepi.2009.01.018
- Ottiger B, Vanbellingen T, Gabriel C, Huberle E, Koenig-Bruhin M, Pflugshaupt T, Bohlhalter S, Nyffeler T. Validation of the new Lucerne ICF-based Multidisciplinary Observation Scale (LIMOS) for stroke patients. *PLoS One*. 2015;10:e0130925. doi: 10.1371/journal.pone.0130925
- Vanbellingen T, Ottiger B, Pflugshaupt T, Mehrholz J, Bohlhalter S, Nef T, Nyffeler T. The responsiveness of the Lucerne ICF-based Multidisciplinary Observation Scale: a comparison with the Functional Independence Measure and the Barthel Index. *Front Neurol*. 2016;7:152. doi: 10.3389/fneur.2016.00152
- Dunn OJ. Multiple comparisons using rank sums. *Technometrics*. 1964;6:241–252. doi: 10.1080/00401706.1964.10490181
- Dahlhaus R. Graphical interaction models for multivariate time series 1. *Metrika*. 2000;51:157–172. doi: 10.1007/s001840000055
- von Elm E, Altman DG, Egger M, Pocock SJ, Gøtzsche PC, Vandenbroucke JP. The Strengthening of Reporting of Observational Studies in Epidemiology (STROBE) statement: guidelines for reporting observational studies. *PLoS Med*. 2007;4:e296. doi: 10.1371/journal.pmed.0040296
- Wilson L, Horton L, Kunzmann K, Sahakian BJ, Newcombe VF, Stamatakis EA, von Steinbüchel N, Cunitz K, Covic A, Maas A, et al. Understanding the relationship between cognitive performance and function in daily life after traumatic brain injury. *J Neurol Neurosurg Psychiatry*. 2020;92:407–417. doi: 10.1136/jnnp-2020-324492
- Argyropoulos GPD, van Dun K, Adamaszek M, Leggio M, Manto M, Masciullo M, Molinari M, Stoodley CJ, Van Overwalle F, Ivry RB, et al. The cerebellar cognitive affective/Schmahmann syndrome: a task force paper. *Cerebellum*. 2020;19:102–125. doi: 10.1007/s12311-019-01068-8
- Garrard P, Bradshaw D, Jäger HR, Thompson AJ, Losseff N, Playford D. Cognitive dysfunction after isolated brain stem insult. An underdiagnosed cause of long term morbidity. *J Neurol Neurosurg Psychiatry*. 2002;73:191–194. doi: 10.1136/jnnp.73.2.191
- Nys GM, van Zandvoort MJ, de Kort PL, Jansen BP, de Haan EH, Kappelle LJ. Cognitive disorders in acute stroke: prevalence and clinical determinants. *Cerebrovasc Dis*. 2007;23:408–416. doi: 10.1159/000101464
- Ten Brink AF, Verwer JH, Biesbroek JM, Visser-Meily JMA, Nijboer TCW. Differences between left- and right-sided neglect revisited: a large cohort study across multiple domains. *J Clin Exp Neuropsychol*. 2017;39:707–723. doi: 10.1080/13803395.2016.1262333
- Embrechts E, Van Crielinge T, Schröder J, Nijboer T, Lafosse C, Truijzen S, Saeys W. The association between visuospatial neglect and balance and mobility post-stroke onset: a systematic review. *Ann Phys Rehabil Med*. 2021;64:101449. doi: 10.1016/j.rehab.2020.10.003
- Doron N, Rand D. Is unilateral spatial neglect associated with motor recovery of the affected upper extremity poststroke? A systematic review. *Neurorehabil Neural Repair*. 2019;33:179–187. doi: 10.1177/1545968319832606
- Güntürkün O, Ströckens F, Ocklenburg S. Brain lateralization: a comparative perspective. *Physiol Rev*. 2020;100:1019–1063. doi: 10.1152/physrev.00006.2019
- Bosch J, Pearce LA, Sharma M, Mikulík R, Whiteley WN, Canavan M, Hart RG, O'Donnell MJ. Functional abilities of an international post-stroke population: Standard Assessment of Global Everyday Activities (SAGEA) scale. *J Stroke Cerebrovasc Dis*. 2022;31:106329. doi: 10.1016/j.jstrokecerebrovasdis.2022.106329
- Chen C, Leys D, Esquenazi A. The interaction between neuropsychological and motor deficits in patients after stroke. *Neurology*. 2013;80:S27–S34. doi: 10.1212/WNL.0b013e3182762569
- Walker CM, Sunderland A, Sharma J, Walker MF. The impact of cognitive impairment on upper body dressing difficulties after stroke: a video analysis of patterns of recovery. *J Neurol Neurosurg Psychiatry*. 2004;75:43–48.

32. Preston E, Ada L, Stanton R, Mahendran N, Dean CM. Prediction of independent walking in people who are nonambulatory early after stroke: a systematic review. *Stroke*. 2021;52:3217–3224. doi: [10.1161/strokeaha.120.032345](https://doi.org/10.1161/strokeaha.120.032345)
33. Rondina JM, Park CH, Ward NS. Brain regions important for recovery after severe post-stroke upper limb paresis. *J Neurol Neurosurg Psychiatry*. 2017;88:737–743. doi: [10.1136/jnnp-2016-315030](https://doi.org/10.1136/jnnp-2016-315030)
34. Janacsek K, Evans TM, Kiss M, Shah L, Blumenfeld H, Ullman MT. Subcortical cognition: the fruit below the rind. *Annu Rev Neurosci*. 2022;45:361–386. doi: [10.1146/annurev-neuro-110920-013544](https://doi.org/10.1146/annurev-neuro-110920-013544)
35. Vanbellingen T, Ottiger B, Maaijwee N, Pflugshaupt T, Bohlhalter S, Müri RM, Nef T, Cazzoli D, Nyffeler T. Spatial neglect predicts upper limb use in the activities of daily living. *Cerebrovasc Dis*. 2017;44:122–127. doi: [10.1159/000477500](https://doi.org/10.1159/000477500)
36. Ford A, Dougalas J, O'Halloran R. The experience of close personal relationships from the perspective of people with aphasia: thematic analysis of the literature. *Aphasiology*. 2018;23:367–393. doi: [10.1080/02687038.2017.1413486](https://doi.org/10.1080/02687038.2017.1413486)
37. Carragher M, Steel G, O'Halloran R, Torabi T, Johnson H, Taylor NF, Rose M. Aphasia disrupts usual care: the stroke team's perceptions of delivering healthcare to patients with aphasia. *Disabil Rehabil*. 2021;43:3003–3014. doi: [10.1080/09638288.2020.1722264](https://doi.org/10.1080/09638288.2020.1722264)
38. Dunn LE, Schweber AB, Manson DK, Lendaris A, Herber C, Marshall RS, Lazar RM. Variability in motor and language recovery during the acute stroke period. *Cerebrovasc Dis Extra*. 2016;6:12–21. doi: [10.1159/000444149](https://doi.org/10.1159/000444149)
39. Lyden P, Claesson L, Havstad S, Ashwood T, Lu M. Factor analysis of the National Institutes of Health Stroke Scale in patients with large strokes. *Arch Neurol*. 2004;61:1677–1680. doi: [10.1001/archneur.61.11.1677](https://doi.org/10.1001/archneur.61.11.1677)
40. Moore MJ, Vancleef K, Shalev N, Husain M, Demeyere N. When neglect is neglected: NIHSS observational measure lacks sensitivity in identifying post-stroke unilateral neglect. *J Neurol Neurosurg Psychiatry*. 2019;90:1070–1071. doi: [10.1136/jnnp-2018-319668](https://doi.org/10.1136/jnnp-2018-319668)
41. Brillinger DR. Time series: data analysis and theory, classics in applied mathematics. Society for Industrial and Applied Mathematics. 2001. doi: [10.1137/1.9780898719246](https://doi.org/10.1137/1.9780898719246)
42. Lauritzen SL. *Graphical Models*. Clarendon Press; 1996.
43. Stoica P, Moses RL. *Spectral Analysis of Signals*. Pearson/Prentice Hall; 2005.
44. Efron B, Tibshirani RJ. *An Introduction to the Bootstrap*. Chapman and Hall/CRC; 1994. doi: [10.1201/9780429246593](https://doi.org/10.1201/9780429246593)

SUPPLEMENTAL MATERIAL

Data S1.

A. Supplemental Methods and Results

A.1 Information on rehabilitation content

Patients received personalized multidisciplinary neurorehabilitation, including occupational therapy, physical therapy, rehabilitative nursing, speech and language therapy, and neuropsychology. The focus and composition depended on the limitations and restrictions of the patient.

The therapies were mainly problem- and task-oriented, were repetitive of nature and principles of motor learning were applied.

A.2 Graphical Models

Let $X[\cdot]$ be stochastic process with n components, i.e. $X[t] \in \mathbb{R}^n$. We aim to visualize whether a pair $a, b \in \{1, \dots, n\}$ of components of $X[\cdot]$ has a relationship, when linearly accounting for past, present and future observed values in another set $S \subset \{1, \dots, n\}$ of components. I.e., we want to answer the following question: *Assume that we observe $X_S[\cdot]$, the evolution of the stochastic process components in the set S , and use this information to predict $X_a[\cdot]$, the evolution of component a , then does also observing component $X_b[\cdot]$ provide additional information?*

To this end we compute a graph (where the nodes correspond to the n components of X) such that we can answer the above question simply by checking whether there is a path between a and b in the graph that does not contain any node in S .

The purpose of this appendix is to give a self-contained explanation of the necessary theory. Specifically, we collect the relevant results from the literature^{19,41,42}, and provide detailed proofs thereof. First, we introduce background on Fourier analysis in Section A.2.1 and provide the definition and useful properties of the class of stochastic processes we consider in Section A.2.2. In Section A.2.3 we then make the above notion of linear relationships precise. Finally, in Section A.2.4, we define the mentioned graphical representation and prove its properties.

Notation For $n_1, n_2 \in \mathbb{N}$, we denote by $(\mathbb{R}^{n_1})^{\mathbb{Z}}$ the set of all sequences of n_1 -dimensional vectors, and by $(\mathbb{R}^{n_1 \times n_2})^{\mathbb{Z}}$ the set of all sequences of $n_1 \times n_2$ -dimensional matrices. For matrices $M_1, M_2 \in \mathbb{R}^{n_1 \times n_2}$ we use the notation $M_1 \succ M_2$ or $M_1 \succcurlyeq M_2$ to indicate that the matrix $M_1 - M_2$ is positive definite or semi-definite, respectively. By $|M_1|$ we denote the sum of the absolute values of the entries in the matrix M_1 . By $M_1^H = \overline{M_1}^T$ we denote the Hermitian transpose of M_1 .

A.2.1 Preliminaries

We start by defining the space of absolutely summable matrix sequences as follows.

Definition S1. For $n_1, n_2 \in \mathbb{N}$ we define the space of absolutely summable matrix sequences as

$$\ell^1(\mathbb{R}^{n_1 \times n_2}) := \left\{ x[\cdot] \mid x \in (\mathbb{R}^{n_1 \times n_2})^{\mathbb{Z}}, \sum_{t=-\infty}^{\infty} |x[t]| < \infty \right\},$$

where $|x[t]|$ denotes the sum of the absolute values of the entries in $x[t]$, i.e. $|x[t]| = \sum_{j=1}^{n_1} \sum_{\ell=1}^{n_2} |x_{j\ell}[t]|$.

A core building block of the theory is the ability to produce a time-series from another time-series using a linear operation. To this end, we define convolution operation for matrix sequences.

Definition S2 (Convolution). Let $x[\cdot] \in \ell^1(\mathbb{R}^{n_1 \times n_2})$ and $y[\cdot] \in (\mathbb{R}^{n_2 \times n_3})^{\mathbb{Z}}$. We define the convolution according to

$$(x * y)[t] = \sum_{\ell=-\infty}^{\infty} x[\ell]y[t - \ell].$$

A further core tool is the Fourier transform, defined as follows.

Definition S3 (Discrete time Fourier transform). Let $x[\cdot] \in \ell^1(\mathbb{R}^{n_1 \times n_2})$ we define

$$\mathcal{F}\{x\}(\alpha) = \sum_{t=-\infty}^{\infty} x[t]e^{-2i\pi t\alpha} =: f(\alpha),$$

where $\alpha \in [0, 1]$. The inverse transform of $f(\alpha)$ is given by

$$\mathcal{F}^{-1}\{f\}[t] = \int_0^1 f(\alpha)e^{2i\pi t\alpha} d\alpha = x[t],$$

with $t \in \mathbb{Z}$.

This allows us to express the convolution as a simple product in frequency space. First, we verify that $\mathcal{F}\{x * y\}$ is well-defined, which requires $x * y$ to be summable.

Lemma S4. Let $x[\cdot] \in \ell^1(\mathbb{R}^{n_1 \times n_2})$ and $y[\cdot] \in \ell^1(\mathbb{R}^{n_2 \times n_3})$, then

$$x * y \in \ell^1(\mathbb{R}^{n_1 \times n_3})$$

Proof.

$$\begin{aligned} \sum_{t=-\infty}^{\infty} |(x * y)[t]| &\leq \sum_{t=-\infty}^{\infty} \sum_{\ell=-\infty}^{\infty} |x[\ell]y[t - \ell]| \\ &\leq (n_1 \cdot n_2 \cdot n_3) \sum_{\ell=-\infty}^{\infty} |x[\ell]| \sum_{t=-\infty}^{\infty} |y[t - \ell]| < \infty \end{aligned}$$

□

Now we can state the convolution theorem.

Theorem S5 (Convolution theorem). Let $n_1, n_2, n_3 \in \mathbb{N}$, $x \in \ell^1(\mathbb{R}^{n_1 \times n_2})$, and $y \in \ell^1(\mathbb{R}^{n_2 \times n_3})$. We have

$$\mathcal{F}\{x * y\}(\alpha) = \mathcal{F}\{x\}(\alpha) \mathcal{F}\{y\}(\alpha).$$

Proof.

$$\begin{aligned}
 \mathcal{F}\{x * y\}(\alpha) &= \sum_{t=-\infty}^{\infty} \sum_{\ell=-\infty}^{\infty} x[\ell]y[t-\ell]e^{-2i\pi t\alpha} \\
 &= \sum_{\ell=-\infty}^{\infty} x[\ell] \sum_{t=-\infty}^{\infty} y[t-\ell]e^{-2i\pi t\alpha} \\
 &= \sum_{\ell=-\infty}^{\infty} x[\ell] \sum_{t'=-\infty}^{\infty} y[t']e^{-2i\pi(t'+\ell)\alpha} \\
 &= \sum_{\ell=-\infty}^{\infty} x[\ell]e^{-2i\pi\ell\alpha} \mathcal{F}\{y\}(\alpha) \\
 &= \mathcal{F}\{x\}(\alpha) \mathcal{F}\{y\}(\alpha).
 \end{aligned}$$

□

We conclude our introduction to harmonic analysis with the following lemma, that we will need later.

Lemma S6. Let $x[\cdot] \in \ell^1(\mathbb{R}^{n_1 \times n_2})$ and define $x'[t] = x[-t]^T$. We have

$$\mathcal{F}\{x'\} = \mathcal{F}\{x\}^H.$$

Proof. We compute

$$\begin{aligned}
 \mathcal{F}\{x'\}(\alpha) &= \sum_{t=-\infty}^{\infty} (x[-t]^T)e^{-2i\pi t\alpha} \\
 &= \sum_{t=-\infty}^{\infty} (x[t]^T)e^{2i\pi t\alpha} \\
 &= \overline{\left(\sum_{t=-\infty}^{\infty} (x[t]^T)e^{-2i\pi t\alpha} \right)} \\
 &= \overline{\mathcal{F}\{x\}(\alpha)^T} = (\mathcal{F}\{x\})^H,
 \end{aligned} \tag{1}$$

where in (1) we use that $x[t] \in \mathbb{R}^{n_1 \times n_2}, \forall t \in \mathbb{Z}$. □

Apart from the above background in harmonic analysis, we will need the following result from linear algebra regarding the inversion of a block matrix.

Theorem S7 (Schur Complement). Let $M \in \mathbb{C}^{n_1 \times n_2}$ be a non-singular block matrix

$$M = \begin{pmatrix} A & B \\ C & D \end{pmatrix}$$

such that D is non-singular as well. Then

$$M^{-1} = \begin{pmatrix} E^{-1} & -E^{-1}F \\ -GE^{-1} & D^{-1} + GE^{-1}F \end{pmatrix} \tag{2}$$

where $E = A - BD^{-1}C$, $F = BD^{-1}$, and $G = D^{-1}C$ with E non-singular.

Proof. Through direct verification we see that M can be written as

$$M = \begin{pmatrix} A & B \\ C & D \end{pmatrix} = \begin{pmatrix} I & F \\ 0 & I \end{pmatrix} \begin{pmatrix} E & 0 \\ 0 & D \end{pmatrix} \begin{pmatrix} I & 0 \\ G & I \end{pmatrix} \tag{3}$$

and thus

$$\det(M) = \det \begin{pmatrix} I & F \\ 0 & I \end{pmatrix} \det \begin{pmatrix} E & 0 \\ 0 & D \end{pmatrix} \det \begin{pmatrix} I & 0 \\ G & I \end{pmatrix} = \det(E) \det(D).$$

Since M and D are both non-singular by assumption this implies $\det(E) \neq 0$, i.e., E is non-singular as well. Hence, we can invert (3) as follows

$$M^{-1} = \begin{pmatrix} I & 0 \\ G & I \end{pmatrix}^{-1} \begin{pmatrix} E & 0 \\ 0 & D \end{pmatrix}^{-1} \begin{pmatrix} I & F \\ 0 & I \end{pmatrix}^{-1} = \begin{pmatrix} I & 0 \\ -G & I \end{pmatrix} \begin{pmatrix} E^{-1} & 0 \\ 0 & D^{-1} \end{pmatrix} \begin{pmatrix} I & -F \\ 0 & I \end{pmatrix} \quad (4)$$

Simplifying (4), we obtain (2). \square

A.2.2 Stationary stochastic processes

We now introduce the stochastic processes under consideration and derive some basic properties.

Definition S8 (Wide sense stationary). Let $X[\cdot]$ be an n -dimensional stochastic process indexed by $t \in \mathbb{Z}$, i.e. $X[t] \in \mathbb{R}^n$, $\forall t \in \mathbb{Z}$. X is wide-sense stationary (WSS) if there is an $m_X \in \mathbb{R}^n$, which we call the mean of X , such that

$$\mathbb{E}[X[t]] = m_X, \quad \forall t \in \mathbb{Z}$$

and a sequence $k_X[\cdot] \in \ell^1(\mathbb{R}^{n \times n})$, which we call the autocovariance sequence of X , such that

$$\mathbb{E}[X[t]X[t']^T] = k_X[t - t'], \quad \forall t, t' \in \mathbb{Z}. \quad (5)$$

Remark S9. Since (5) only depends on the difference $t - t'$ we can set $t' = 0$ and calculate the autocovariance sequence according to

$$k_X[\tau] = \mathbb{E}[X[\tau]X[0]^T], \quad \forall \tau \in \mathbb{Z}.$$

Remark S10. Let $X[\cdot]$ be a stochastic process as in Definition S8. We have

$$k_X[\tau] = \mathbb{E}[X[\tau]X[0]^T] = \mathbb{E}[X[0]X[\tau]^T]^T = k_X[-\tau]^T.$$

Remark S11. Let $X[\cdot]$ be a stochastic process as in Definition S8, and set $f(\alpha) := \mathcal{F}\{k_X\}(\alpha)$. Then, from Remark S10 and Lemma S6 it follows that $f(\alpha) = f(\alpha)^H$ for all $\alpha \in [0, 1]$.

$f = \mathcal{F}\{k_X\}$ is called the power spectral density of X . This matrix valued function is positive semidefinite as we show in the following Lemma.

Lemma S12. Let $X[\cdot]$ be a stochastic process as in Definition S8, and $f = \mathcal{F}\{k_X\}$. Then $f(\alpha)$ is positive semidefinite for all $\alpha \in [0, 1]$.

Proof. Fix $\alpha \in [0, 1]$ arbitrarily and define for, $T \in \mathbb{N}$,

$$I_T := \frac{1}{T} \begin{pmatrix} \sum_{t=0}^{T-1} X[t]e^{-2i\pi t\alpha} \\ \sum_{\ell=0}^{T-1} X[\ell]e^{-2i\pi \ell\alpha} \end{pmatrix}^H,$$

which is positive semidefinite by construction. Thus, $\mathbb{E}[I_T]$ is positive semidefinite as well. We next

compute the limit with respect to $T \rightarrow \infty$ of this expression. To this end, we calculate

$$\begin{aligned} \mathbb{E}[I_T] &= \frac{1}{T} \sum_{t=0}^{T-1} \sum_{\ell=0}^{T-1} \mathbb{E}[X[t]X[\ell]^H] e^{-2i\pi(t-\ell)\alpha} \\ &= \frac{1}{T} \sum_{\ell=0}^{T-1} \sum_{t=0}^{T-1} k_X[t-\ell] e^{-2i\pi(t-\ell)\alpha} \\ &= \frac{1}{T} \sum_{\tau=-(T-1)}^{T-1} (T-|\tau|) k_X[\tau] e^{-2i\pi\tau\alpha} \\ &= \sum_{\tau=-(T-1)}^{T-1} k_X[\tau] e^{-2i\pi\tau\alpha} - \frac{1}{T} \sum_{\tau=-(T-1)}^{T-1} |\tau| k_X[\tau] e^{-2i\pi\tau\alpha}. \end{aligned}$$

Now, as $\sum_{\tau=-\infty}^{\infty} |k_X[\tau]| < \infty$ by assumption, $\sum_{\tau=-(T-1)}^{T-1} k_X[\tau] e^{-2i\pi\tau\alpha}$ converges to $f_X(\alpha)$ as $T \rightarrow \infty$. It remains to show that

$$\frac{1}{T} \sum_{\tau=-(T-1)}^{T-1} |\tau| k_X[\tau] e^{-2i\pi\tau\alpha} \xrightarrow{T \rightarrow \infty} 0. \quad (6)$$

To establish this, fix $\epsilon > 0$ and observe that $\exists T_0 \in \mathbb{N}$ such that $\sum_{\tau \in \mathbb{Z}, |\tau| > T_0} |k_X[\tau]| < \epsilon$. Now, for $T > T_0$,

$$\begin{aligned} \left| \frac{1}{T} \sum_{\tau=-(T-1)}^{T-1} |\tau| k_X[\tau] e^{-2i\pi\tau\alpha} \right| &\leq \frac{1}{T} \sum_{\tau=-(T-1)}^{T-1} |\tau k_X[\tau] e^{-2i\pi\tau\alpha}| \\ &= \frac{1}{T} \sum_{\tau=-(T_0-1)}^{T_0-1} |\tau k_X[\tau]| + \sum_{\tau \in \mathbb{Z}, T_0 \leq |\tau| < T} \frac{|\tau|}{T} |k_X[\tau]| \\ &\leq \frac{1}{T} \sum_{\tau=-(T_0-1)}^{T_0-1} T_0 C + \sum_{\tau \in \mathbb{Z}, T_0 \leq |\tau| < T} |k_X[\tau]| \\ &\leq \frac{2T_0^2 C}{T} + \sum_{\tau \in \mathbb{Z}, T_0 \leq |\tau|} |k_X[\tau]| \\ &\leq \frac{2T_0^2 C}{T} + \epsilon \xrightarrow{T \rightarrow \infty} \epsilon, \end{aligned}$$

where $C = \sup_{\tau \in \mathbb{Z}} |k_X[\tau]| < \infty$. Since we can choose ϵ arbitrarily small, this yields (6). Thus, we have established

$$f_X(\alpha) = \lim_{T \rightarrow \infty} \underbrace{\mathbb{E}[I_T]}_{\geq 0} \geq 0.$$

As α was arbitrary, this completes the proof. \square

We shall place some additional conditions on the WSS processes we consider. These are specified in the following definition.

Definition S13. We say that a stochastic process $X[\cdot]$ is zero-mean, WSS and non-degenerate if it satisfies Definition S8 such that $m_X = 0$ and $\mathcal{F}\{k_X\}(\alpha)$ is non-singular $\forall \alpha \in [0, 1]$.

The zero-mean condition is purely for convenience, while requiring the power spectral density to be non-singular excludes certain degenerate cases. For example this condition would be violated, if two components of the stochastic process are always identical.

With this definition we get the following corollary of Lemma S12.

Corollary S14. Let $X[\cdot]$ be an n -dimensional stochastic process satisfying Definition S13, where $f = \mathcal{F}\{k_X\}$. Then for any subset $A \subset [n]$ and $\forall \alpha \in [0, 1]$ the principal submatrix $f_{AA}(\alpha)$, which is obtained from $f(\alpha)$ by taking only those rows and columns with indices in the set A , is positive definite and thus non-singular.

Proof. Fix α arbitrarily. By Lemma S12, $f(\alpha)$ is positive semi-definite and thus has only non-negative eigenvalues. Since $f(\alpha)$ is non-singular by assumption, zero is not an eigenvalue. Therefore, $f(\alpha) \succ 0$, i.e. $\forall v \in \mathbb{C}^n$ we have $v^H f(\alpha)v > 0$. Now let $w \in \mathbb{C}^{|A|}$ be arbitrary and fix $v \in \mathbb{C}^n$ such that $v_A = w$ and $v_{A^c} = 0$. We get

$$w^H (f_{AA}(\alpha))w = v^H f(\alpha)v > 0,$$

which, since w is arbitrary, yields $f_{AA}(\alpha) \succ 0$. \square

A.2.3 Linear relationships

Now we consider a particular n -dimensional stochastic process $X[\cdot]$. Thus, we shall frequently omit the explicit dependency on X in our notation. We use the capital letters $A, B \subset [n]$ to denote subsets of the components of the stochastic process. E.g. $X_A[\cdot]$ corresponds to the $|A|$ -dimensional vector process containing only the components corresponding to the indices in the set $A \subset \{1, \dots, n\}$. Similarly, for disjoint $A, B \subset [n]$, we shall identify components of the autocovariance sequence $k_X[\tau]$ as follows,

$$\begin{aligned} c_{AA}[\tau] &:= \mathbb{E}[X_A[\tau]X_A[0]^T], & c_{BB}[\tau] &:= \mathbb{E}[X_B[\tau]X_B[0]^T], \\ c_{AB}[\tau] &:= \mathbb{E}[X_A[\tau]X_B[0]^T], & c_{BA}[\tau] &:= \mathbb{E}[X_B[\tau]X_A[0]^T]. \end{aligned} \quad (7)$$

Furthermore, we identify components of $f = \mathcal{F}\{k_X\}$, the power spectral density, as follows

$$\begin{aligned} f_{AA}(\alpha) &:= \mathcal{F}\{c_{AA}\}(\alpha), & f_{BB}(\alpha) &:= \mathcal{F}\{c_{BB}\}(\alpha), \\ f_{AB}(\alpha) &:= \mathcal{F}\{c_{AB}\}(\alpha), & f_{BA}(\alpha) &:= \mathcal{F}\{c_{BA}\}(\alpha). \end{aligned}$$

Remark S15. From Remark S10 we have

$$c_{BB}[\tau] = c_{BB}[-\tau]^T \quad \text{and} \quad c_{BA}[\tau] = c_{AB}[-\tau]^T,$$

and, from Remark S11, we have

$$f_{BB}(\alpha) = f_{BB}(\alpha)^H \quad \text{and} \quad f_{BA}(\alpha) = f_{AB}(\alpha)^H.$$

We are interested in linearly predicting the evolution of some components from the observed time-series corresponding to other components. This linear prediction of a time-series based on values of another time-series can be expressed through convolution. It is parametrized by a matrix sequence $\beta[\cdot]$, which is used in the convolution, and a mean vector μ .

Definition S16. Let $X[\cdot]$ be an n -dimensional, stochastic process satisfying Definition S13. Let $A, B \subset [n]$ be non-empty disjoint sets. For $\mu \in \mathbb{R}^{|A|}$ and $\beta[\cdot] \in \ell^1(\mathbb{R}^{|A| \times |B|})$, we define the following parametrized prediction

$$\tilde{X}_{A,B}^{\mu,\beta}[t] := \mu + \sum_{\ell=-\infty}^{\infty} \beta[\ell]X_B[t-\ell].$$

We define the error incurred by this predictor according to

$$\tilde{E}_{A,B}^{\mu,\beta}[t] := X_A[t] - \tilde{X}_{A,B}^{\mu,\beta}[t]. \quad (8)$$

Note that both $\tilde{X}_{A,B}^{\mu,\beta}$ and $\tilde{E}_{A,B}^{\mu,\beta}$ are again stochastic processes, which, as we now see, satisfy Definition S8.

Theorem S17. Let $X[\cdot]$ be an n -dimensional, stochastic process satisfying Definition S13. Let $A, B \subset [n]$ be non-empty disjoint sets. Let $\mu \in \mathbb{R}^{|A|}$ and $\beta[\cdot] \in \ell^1(\mathbb{R}^{|A| \times |B|})$. Then, the process $\tilde{E}_{A,B}^{\mu,\beta}$ defined in (8) satisfies Definition S8. Its mean is given by

$$\mathbb{E} \left[\tilde{E}_{A,B}^{\mu,\beta}[t] \right] = \mu, \quad \forall t \in \mathbb{Z} \quad (9)$$

and its autocovariance sequence, using the notation (7), by

$$\mathbb{E} \left[\tilde{E}_{A,B}^{\mu,\beta}[t] \tilde{E}_{A,B}^{\mu,\beta}[t']^T \right] = \mu\mu^T + c_{AA}[t-t'] - (c_{AB} * \beta')[t-t'] - (\beta * c_{BA})[t-t'] + (\beta * c_{BB} * \beta')[t-t'], \quad (10)$$

$\forall t, t' \in \mathbb{Z}$, where $\beta'[t] := \beta[-t]^T$.

Proof. To establish (9) we first use $\mathbb{E}[X[t]] = m_X = 0$, $\forall t \in \mathbb{Z}$ and compute

$$\begin{aligned} \mathbb{E} \left[\tilde{E}_{A,B}^{\mu,\beta}[t] \right] &= \mathbb{E} \left[X_A[t] - \mu - \sum_{\ell=-\infty}^{\infty} \beta[\ell] X_B[t-\ell] \right] \\ &= \mathbb{E} [X_A[t]] - \mu - \sum_{\ell=-\infty}^{\infty} \beta[\ell] \mathbb{E} [X_B[t-\ell]] \\ &= \mu, \quad \forall t \in \mathbb{Z}. \end{aligned}$$

Next, fix $t, t' \in \mathbb{Z}$ arbitrarily and let $\Delta := t - t'$. We compute

$$\begin{aligned} \mathbb{E} \left[\tilde{E}_{A,B}^{\mu,\beta}[t] \tilde{E}_{A,B}^{\mu,\beta}[t']^T \right] &= \mathbb{E} \left[\underbrace{X_A[t] - \sum_{\ell=-\infty}^{\infty} \beta[\ell] X_B[t-\ell] - \mu}_{=: Z[t]} \right] \left[\underbrace{X_A[t'] - \sum_{\ell'=-\infty}^{\infty} \beta[\ell'] X_B[t'-\ell'] - \mu}_{=: Z[t']} \right]^T \\ &= \mathbb{E} [Z[t] Z[t']^T] + \mu\mu^T, \end{aligned} \quad (11)$$

where we use that the cross terms evaluate to zero because $\mathbb{E}[Z[t]] = 0$ as we have seen before. Further, we calculate

$$\begin{aligned} \mathbb{E} [Z[t] Z[t']^T] &= \mathbb{E} [X_A[t] X_A[t']^T] - \sum_{\ell=-\infty}^{\infty} \beta[\ell] \mathbb{E} [X_B[t-\ell] X_A[t']^T] \\ &\quad - \sum_{\ell'=-\infty}^{\infty} \mathbb{E} [X_A[t] X_B[t'-\ell']^T] \beta[\ell']^T + \sum_{\ell=-\infty}^{\infty} \sum_{\ell'=-\infty}^{\infty} \beta[\ell] \mathbb{E} [X_B[t-\ell] X_B[t'-\ell']^T] \beta[\ell']^T \\ &= c_{AA}[t-t'] - \sum_{\ell=-\infty}^{\infty} \beta[\ell] c_{BA}[t-t'-\ell] \\ &\quad - \sum_{\ell'=-\infty}^{\infty} c_{AB}[t-t'+\ell'] \beta[\ell']^T + \sum_{\ell=-\infty}^{\infty} \beta[\ell] \sum_{\ell'=-\infty}^{\infty} c_{BB}[t-t'+\ell'-\ell] \beta[\ell']^T \\ &= c_{AA}[\Delta] - \sum_{\ell=-\infty}^{\infty} \beta[\ell] c_{BA}[\Delta-\ell] \\ &\quad - \underbrace{\sum_{\ell'=-\infty}^{\infty} c_{AB}[\Delta+\ell'] \beta[\ell']^T}_{=\sum_{\ell'=-\infty}^{\infty} c_{AB}[\ell] \beta[-(\Delta-\ell)]^T} + \sum_{\ell=-\infty}^{\infty} \beta[\ell] \underbrace{\sum_{\ell'=-\infty}^{\infty} c_{BB}[\Delta+\ell'-\ell] \beta[\ell']^T}_{=\sum_{\ell''=-\infty}^{\infty} c_{BB}[\ell''] \beta[-((\Delta-\ell)-\ell'')]^T} \\ &= c_{AA}[\Delta] - (\beta * c_{BA})[\Delta] - (c_{AB} * \beta')[\Delta] + \underbrace{\sum_{\ell=-\infty}^{\infty} \beta[\ell] (c_{BB} * \beta')[\Delta-\ell]}_{(\beta * c_{BB} * \beta')[\Delta]} \end{aligned} \quad (12)$$

Together, (11) and (12) imply (10). Finally, from (9), (10) and Lemma S4, it follows that $\tilde{E}_{A,B}^{\mu,\beta}$ satisfies Definition S8. \square

In light of the previous theorem we use the following notation for the covariance sequence of the error process, i.e. the quantity in (10),

$$\tilde{e}_{A,B}^{\mu,\beta}[\tau] := \mathbb{E} \left[\tilde{E}_{A,B}^{\mu,\beta}[\tau] \tilde{E}_{A,B}^{\mu,\beta}[0]^T \right].$$

Now we want to pick μ^* and β^* that are optimal in the sense that $\tilde{e}_{A,B}^{\mu,\beta}[0] \succcurlyeq \tilde{e}_{A,B}^{\mu^*,\beta^*}[0]$ for all other choices μ and β . Corollary S19 below then shows, that with this criterion also the expected squared error in each component is minimized.

Theorem S18. *Let $X[\cdot]$ be an n -dimensional, stochastic process satisfying Definition S13 and let $f = \mathcal{F}\{k_X\}$. Further, let $A, B \subset [n]$ be non-empty disjoint sets. Then for all $\mu \in \mathbb{R}^{|A|}$ and $\beta[\cdot] \in \ell^1(\mathbb{R}^{|A| \times |B|})$ we have*

$$\tilde{e}_{A,B}^{\mu,\beta}[0] \succcurlyeq \int_0^1 (f_{AA}(\alpha) - f_{AB}(\alpha)f_{BB}(\alpha)^{-1}f_{BA}(\alpha)) d\alpha \quad (13)$$

with equality for $\mu^* = 0$ and $\beta^* = \mathcal{F}^{-1}\{f_{AB}(\alpha)f_{BB}(\alpha)^{-1}\}$. We call the error process with this optimal choice

$$E_{A,B} := E_{A,B}^{\mu^*,\beta^*} \quad (14)$$

and its autocovariance sequence

$$e_{A,B} := \tilde{e}_{A,B}^{\mu^*,\beta^*}.$$

The power spectral density is then given by

$$\mathcal{F}\{e_{A,B}\}(\alpha) = f_{AA}(\alpha) - f_{AB}(\alpha)f_{BB}^{-1}(\alpha)f_{BA}(\alpha). \quad (15)$$

Proof. We denote $\hat{\beta} = \mathcal{F}\{\beta\}$ and apply the Fourier transform to (10) as follows

$$\begin{aligned} \mathcal{F}\{\tilde{e}_{A,B}^{\mu,\beta}\}(\alpha) &= \mathcal{F}\{\mu\mu^T + c_{AA} - (c_{AB} * \beta') - (\beta * c_{BA}) + (\beta * c_{BB} * \beta')\} \\ &= \mu\mu^T + f_{AA}(\alpha) - f_{AB}(\alpha)\hat{\beta}(\alpha)^H - \hat{\beta}(\alpha)f_{BA}(\alpha) + \hat{\beta}(\alpha)f_{BB}(\alpha)\hat{\beta}(\alpha)^H \end{aligned} \quad (16)$$

$$\begin{aligned} &= \mu\mu^T + f_{AA} - f_{AB}(f_{BB}^{-1}f_{BB}^H)\hat{\beta}^H - \hat{\beta}f_{AB}^H + \hat{\beta}f_{BB}f_{BB}^{-1}f_{BB}^H\hat{\beta}^H \\ &\quad - f_{AB}f_{BB}^{-1}f_{BA} + f_{AB}f_{BB}^{-1}f_{AB}^H \end{aligned} \quad (17)$$

$$\begin{aligned} &= \mu\mu^T + (f_{AA}(\alpha) - f_{AB}(\alpha)f_{BB}^{-1}(\alpha)f_{BA}(\alpha)) \\ &\quad + \left(\hat{\beta}(\alpha)f_{BB}(\alpha) - f_{AB}(\alpha) \right) f_{BB}^{-1}(\alpha) \left(\hat{\beta}(\alpha)f_{BB}(\alpha) - f_{AB}(\alpha) \right)^H, \end{aligned} \quad (18)$$

where in (16) we use Lemma S6 and in (17) we use the symmetry properties from Remark S15 while omitting the explicit dependence on α to keep notation more concise.

Next we show that

$$\left(\hat{\beta}(\alpha)f_{BB}(\alpha) - f_{AB}(\alpha) \right) f_{BB}^{-1}(\alpha) \left(\hat{\beta}(\alpha)f_{BB}(\alpha) - f_{AB}(\alpha) \right)^H \succcurlyeq 0, \quad \forall \alpha \in [0, 1]. \quad (19)$$

To verify this, fix $\alpha \in [0, 1]$ arbitrarily and let $v \in \mathbb{C}^{1 \times |A|}$. We compute

$$\begin{aligned} &v \underbrace{\left(\hat{\beta}(\alpha)f_{BB}(\alpha) - f_{AB}(\alpha) \right) f_{BB}^{-1}(\alpha)}_{=:w} \underbrace{\left(\hat{\beta}(\alpha)f_{BB}(\alpha) - f_{AB}(\alpha) \right)^H}_{=:w^H} v^H \\ &= vw (f_{BB}^{-1}f_{BB}) f_{BB}^{-1} (f_{BB}^{-1}f_{BB})^H w^H v^H \\ &= (vwf_{BB}^{-1}) f_{BB}f_{BB}^{-1}f_{BB}^H(f_{BB}^{-1})^H w^H v^H \\ &= (vwf_{BB}^{-1}) f_{BB}(vwf_{BB}^{-1})^H \geq 0, \end{aligned} \quad (20)$$

where in (20) we use that, by Corollary S14, $f_{BB}(\alpha)$ is positive semidefinite. As α was arbitrary, this establishes (19).

Starting from (18), we now use the inverse transform to compute

$$\begin{aligned}\tilde{e}_{A,B}^{\mu,\beta}[0] &= \mathcal{F}^{-1} \left\{ \mathcal{F} \left\{ \tilde{e}_{A,B}^{\mu,\beta} \right\} \right\} [0] \\ &= \mu\mu^T + \int_0^1 (f_{AA}(\alpha) - f_{AB}(\alpha)f_{BB}^{-1}(\alpha)f_{BA}(\alpha)) d\alpha \\ &\quad + \int_0^1 \left(\hat{\beta}(\alpha)f_{BB}(\alpha) - f_{AB}(\alpha) \right) f_{BB}^{-1}(\alpha) \left(\hat{\beta}(\alpha)f_{BB}(\alpha) - f_{AB}(\alpha) \right)^H d\alpha \\ &\succcurlyeq \int_0^1 (f_{AA}(\alpha) - f_{AB}(\alpha)f_{BB}^{-1}(\alpha)f_{BA}(\alpha)) d\alpha,\end{aligned}\tag{21}$$

where in (21) we use $\mu\mu^T \succcurlyeq 0$ as well as (19). This completes the proof of (13). Next, we note that by 41(Theorem 3.8.3) and Lemma S4 it holds that $\mathcal{F}^{-1} \{ f_{AB}(\alpha)f_{BB}(\alpha)^{-1} \} \in \ell^1(\mathbb{R}^{|A| \times |B|})$. Further, with the choice $\beta^* = \mathcal{F}^{-1} \{ f_{AB}(\alpha)f_{BB}(\alpha)^{-1} \}$ the quantity in (19) evaluates to 0, thus, together with $\mu^* = 0$, yielding equality in (13). Finally, inserting the μ^* and β^* in (18) yields (15), which completes the proof. \square

The following corollary gives a practical interpretation to Theorem S18.

Corollary S19. *The choice μ^*, β^* from Theorem S18 also minimizes the mean squared error of each component. That is, $\forall a \in \{1, \dots, |A|\}$*

$$\mathbb{E} \left[(\tilde{E}_{A,B}^{\mu,\beta}[t])_a^2 \right] \geq \mathbb{E} \left[(E_{A,B}[t])_a^2 \right] \quad \forall t \in \mathbb{Z}.\tag{22}$$

Proof. Fix $a \in \{1, \dots, |A|\}$. We first note, that

$$\mathbb{E} \left[(E_{A,B}[t])_a^2 \right] = (e_{A,B}[0])_{aa} \quad \text{and} \quad \mathbb{E} \left[(\tilde{E}_{A,B}^{\mu,\beta}[t])_a^2 \right] = (\tilde{e}_{A,B}^{\mu,\beta}[0])_{aa}, \quad \forall t \in \mathbb{Z}$$

Further, by Theorem S18, we have $\tilde{e}_{A,B}^{\mu,\beta}[0] \succcurlyeq e_{A,B}[0]$, which, by definition, implies that $\tilde{e}_{A,B}^{\mu,\beta}[0] - e_{A,B}[0]$ is positive semidefinite. Let now $v \in \mathbb{C}^{1 \times |A|}$ be the vector, that has a single 1 at the a -th position and is zero otherwise. We have

$$0 \leq v \left(\tilde{e}_{A,B}^{\mu,\beta}[0] - e_{A,B}[0] \right) v^H = (\tilde{e}_{A,B}^{\mu,\beta}[0])_{aa} - (e_{A,B}[0])_{aa}$$

and (22) follows. \square

We proceed to study further properties of the error process $E_{A,B}[\cdot]$ defined in (14). First we show, that this stochastic process also satisfies the conditions of Definition S13.

Corollary S20. *Let $X[\cdot]$ be an n -dimensional, stochastic process satisfying Definition S13. Let $A, B \subset [n]$ be non-empty disjoint sets. Then $E_{A,B}[\cdot]$, as defined in Theorem S18, satisfies Definition S13.*

Proof. Since the stochastic process $E_{A,B}[\cdot]$ is a special case of Definition S16 it follows from Theorem S17 that $E_{A,B}[\cdot]$ satisfies Definition S8, with mean $\mathbb{E} [E_{A,B}] = \mu^* = 0$.

It remains to prove that $\mathcal{F} \{ e_{A,B} \} (\alpha)$, which, according to Theorem S18, is given by $\mathcal{F} \{ e_{A,B} \} (\alpha) = f_{AA}(\alpha) - f_{AB}(\alpha)f_{BB}^{-1}(\alpha)f_{BA}(\alpha)$ where $f(\alpha) = \mathcal{F} \{ k_X \}$, is non-singular $\forall \alpha \in [0, 1]$. To show this, we define $C = A \cup B$, fix $\alpha \in [0, 1]$ arbitrarily and denote $f' = f_{CC}(\alpha)$. By Corollary S14 we have $f' \succ 0$. We write the matrix partitioned as follows

$$f' = \begin{array}{|c|c|} \hline f_{AA} & f_{AB} \\ \hline f_{BA} & f_{BB} \\ \hline \end{array},$$

where, by Corollary S14, $f'_{BB} \succ 0$ as well. Hence, by Theorem S7, $f_{AA} - f_{AB}f_{BB}^{-1}f_{BA} = \mathcal{F} \{ e_{A,B} \} (\alpha)$ is indeed non-singular. As α was arbitrary this completes the proof. \square

Next, we investigate the effect of restricting the set A of components to predict.

Corollary S21. *Let $X[\cdot]$ be a stochastic process satisfying Definition S13 and let $A, B \subset [n]$ be disjoint sets. Further, let $A' \subset A$ and let $M \in \{0, 1\}^{|A'| \times |A|}$ be the matrix such that $M_{j\ell} = 1$ iff the j -th element in A' is the ℓ -th element in A and 0 otherwise. Then*

$$E_{A'.B}[t] = ME_{A.B}[t] \quad \forall t \in \mathbb{Z}, \quad (23)$$

$$\text{and} \quad e_{A'.B}[\tau] = Me_{A.B}[\tau]M^T \quad \forall \tau \in \mathbb{Z}. \quad (24)$$

Proof. Let $\beta_A = \mathcal{F}^{-1} \{f_{AB}(\alpha)f_{BB}(\alpha)^{-1}\}$ and $\beta_{A'} = \mathcal{F}^{-1} \{f_{A'B}(\alpha)f_{BB}(\alpha)^{-1}\}$ be the optimal sequences from Theorem S18 that parametrize $E_{A.B}[\cdot]$ and $E_{A'.B}[\cdot]$ respectively. We observe

$$ME_{A.B}[t] = M\beta_A * X_B = \beta_{A'} * X_B = E_{A'.B}[t] \quad \forall t \in \mathbb{Z}$$

which yields (23). Further, we observe

$$\begin{aligned} \mathcal{F} \{Me_{A.B}M^T\}(\alpha) &= Mf_{AA}(\alpha)M^T - Mf_{AB}(\alpha)f_{BB}^{-1}(\alpha)f_{BA}(\alpha)M^T \\ &= f_{A'A'}(\alpha) - f_{A'B}(\alpha)f_{BB}^{-1}(\alpha)f_{BA'}(\alpha) \\ &= \mathcal{F} \{e_{A'.B}\}(\alpha) \quad \forall \alpha \in [0, 1]. \end{aligned}$$

Taking the inverse Fourier transform we obtain (24). \square

Finally, we introduce the *complex-coherency* of two signals.

Remark S22. *As a special case of Theorem S18 we consider predicting one component of X from another, i.e., $A = \{a\}, B = \{b\}$ for $a, b \in [n]$. Then (15) can be written as*

$$\mathcal{F} \{e_{a,b}\}(\alpha) = f_{aa}(\alpha) - \frac{|f_{ab}(\alpha)|^2}{f_{bb}(\alpha)} = (1 - C_{ab}(\alpha)^2) f_{aa}(\alpha),$$

where

$$C_{ab}(\alpha) := \frac{|f_{ab}(\alpha)|}{\sqrt{f_{aa}(\alpha)f_{bb}(\alpha)}}$$

is known as the *complex-coherency*⁴³(Section 1.6.1) of the signals X_a and X_b .

A.2.4 A graphical representation

Now we are ready to graphically visualize whether components of a stochastic process X are linearly related, when accounting for a set of other components. More precisely, we consider a set $S \subset [n]$ and two components $a, b \in [n] \setminus S$. Then we investigate, whether there is still a linear relationship between X_a and X_b after we account for the evolution of X_S . If this is not the case, we consider a and b as unrelated given S , which we write as $a \perp b \mid S$. That is, if we observe a realization of X_S then additionally observing X_a does not provide further (linear) information about the realization of X_b .

Definition S23. *Let $X[\cdot]$ be an n -dimensional, stochastic process satisfying Definition S13. Let $S \subset [n]$ be a non-empty set and $a, b \in [n] \setminus S$. We define the relation*

$$a \perp b \mid S \quad :\Leftrightarrow \quad \mathbb{E}[E_{a,S}[t]E_{b,S}[\ell]] = 0 \quad \forall t, \ell \in \mathbb{Z}.$$

Since we consider stationary processes, the quantity on the right-hand side only depends on the difference $t - \ell$. Therefore, we can prove the following equivalent formulations which are easier to work with.

Lemma S24. Let $X[\cdot]$ be an n -dimensional, stochastic process satisfying Definition S13. Let $S \subset [n]$ be a non-empty set and $a, b \in [n] \setminus S$. We have the following equivalence

$$\begin{aligned} a \perp b \mid S &\Leftrightarrow e_{\{a,b\}.S}[\tau] \text{ is diagonal, } \forall \tau \in \mathbb{Z} \\ &\Leftrightarrow \mathcal{F}\{e_{\{a,b\}.S}\}(\alpha) \text{ is diagonal, } \forall \alpha \in [0, 1] \end{aligned}$$

Proof. Define $M_a = \begin{pmatrix} 1 & 0 \\ & \end{pmatrix}$ and $M_b = \begin{pmatrix} 0 & 1 \\ & \end{pmatrix}$. From Corollary S21 we know that we can write $E_{a.S}[t] = M_a E_{\{a,b\}.S}[t]$ and $E_{b.S}[t] = M_b E_{\{a,b\}.S}[t]$ for all $t \in \mathbb{Z}$. Hence, using that $E_{\{a,b\}.S}$ is stationary, we have

$$\begin{aligned} \mathbb{E}[E_{a.S}[t]E_{b.S}[\ell]] &= \mathbb{E}[M_a E_{\{a,b\}.S}[t] M_b E_{\{a,b\}.S}[\ell]] \\ &= M_a \mathbb{E}[E_{\{a,b\}.S}[t] E_{\{a,b\}.S}[\ell]^T] M_b^T \\ &= M_a (e_{\{a,b\}.S}[t - \ell]) M_b^T \\ &= (e_{\{a,b\}.S}[t - \ell])_{12}, \quad \forall t, \ell \in \mathbb{Z}. \end{aligned}$$

Thus, we have shown that $\mathbb{E}[E_{a.S}[t]E_{b.S}[\ell]] = 0, \forall t, \ell \in \mathbb{Z}$ is equivalent to $(e_{\{a,b\}.S}[\cdot])_{12} \equiv 0$. The latter in turn is equivalent to $\mathcal{F}\{e_{\{a,b\}.S}\}_{12} \equiv 0$. Exchanging the positions of a and b then completes the proof. \square

This definition is the starting point for our graphical representation. Specifically, we define a graph where the nodes correspond to the components of the stochastic process X . Further, any two nodes a and b are connected by an edge unless $a \perp b \mid [n] \setminus \{a, b\}$ is satisfied.

Definition S25 (Partial correlation graph). Let $X[\cdot]$ be an n -dimensional, stochastic process satisfying Definition S13. The corresponding partial correlation graph $\mathcal{G}_X = (\mathcal{V}, \mathcal{E})$ has nodes $\mathcal{V} = [n]$ and edges $\mathcal{E} \subset \mathcal{V} \times \mathcal{V}$ such that

$$(a, b) \notin \mathcal{E} \Leftrightarrow a \perp b \mid [n] \setminus \{a, b\}.$$

The following theorem shows, how we can determine this graph in a computationally efficient way.

Theorem S26. Let $X[\cdot]$ be an n -dimensional, stochastic process satisfying Definition S13 and let $f = \mathcal{F}\{k_X\}$. For all $\alpha \in [0, 1]$ we define $g(\alpha) := f(\alpha)^{-1}$ and

$$d(\alpha) := - \begin{pmatrix} g(\alpha)_{11}^{-1/2} & \dots & 0 \\ \vdots & \ddots & \vdots \\ 0 & \dots & g(\alpha)_{nn}^{-1/2} \end{pmatrix} g(\alpha) \begin{pmatrix} g(\alpha)_{11}^{-1/2} & \dots & 0 \\ \vdots & \ddots & \vdots \\ 0 & \dots & g(\alpha)_{nn}^{-1/2} \end{pmatrix} \quad \forall \alpha \in [0, 1]. \quad (25)$$

Further, let $a, b \in [n]$ and define the $[0, 1] \rightarrow \mathbb{C}^{2 \times 2}$ function $F(\alpha) := \mathcal{F}\{e_{\{a,b\}.[n] \setminus \{a,b\}}(\alpha)$. We have

$$d_{ab}(\alpha) = \frac{F(\alpha)_{12}}{[F_{11}(\alpha)F_{22}(\alpha)]^{1/2}}, \quad (26)$$

and in particular $d_{ab} \equiv 0 \Rightarrow a \perp b \mid [n] \setminus \{a, b\}$.

Proof. We assume without loss of generality that $a = 1$ and $b = 2$. Further, we define the sets $A = \{a, b\}$ and $B = [n] \setminus \{a, b\}$. Now we fix $\alpha \in [0, 1]$ arbitrary and omit the explicit dependency on α in $f(\alpha)$, $g(\alpha)$ and $F(\alpha)$. Further, we partition $f(\alpha)$ according to

$$f = \begin{pmatrix} f_{AA} & f_{AB} \\ f_{BA} & f_{BB} \end{pmatrix}.$$

By definition f and by Corollary S14 also f_{BB} are non-singular. Thus, we can use Theorem S7 to compute the upper left block of the inverse according to

$$g = f^{-1} = \begin{pmatrix} E^{-1} & \cdot \\ \cdot & \cdot \end{pmatrix},$$

where $E = f_{AA} - f_{AB}f_{BB}^{-1}f_{BA}$. By Theorem S18 we recognize

$$F = \mathcal{F}\{e_{A,B}\}(\alpha) = f_{AA} - f_{AB}f_{BB}^{-1}f_{BA} = E.$$

We now write

$$E = \begin{pmatrix} F_{11} & F_{12} \\ F_{21} & F_{22} \end{pmatrix}$$

with inverse

$$E^{-1} = \frac{1}{F_{11}F_{22} - F_{12}F_{21}} \begin{pmatrix} F_{22} & -F_{12} \\ -F_{21} & F_{11} \end{pmatrix} = \begin{pmatrix} g_{11} & g_{12} \\ g_{21} & g_{22} \end{pmatrix},$$

where in the last equality we simply recognized that E^{-1} constitutes the top left block of g . Thus,

$$d_{ab} = d_{12} = -g_{11}^{-1/2} g_{12} g_{22}^{-1/2} = \frac{F_{12}}{[F_{22}F_{11}]^{-1/2}},$$

which, since α was arbitrary, establishes (26).

It remains to show $d_{ab} \equiv 0 \Rightarrow a \perp b \mid [n] \setminus \{a, b\}$. To this end, we note that $d_{ab}(\cdot) \equiv 0$ implies $F_{12}(\cdot) \equiv 0$, which, in turn, implies $(e_{\{a,b\}.[n] \setminus \{a,b\}}[\cdot])_{12} \equiv 0$. Thus, by Remark S10, $e_{\{a,b\}.[n] \setminus \{a,b\}}$ is indeed diagonal. \square

Remark S27. Comparing (26) with Remark S22, we note that d_{ab} is the complex-coherence of the error processes that arise when predicting a and b separately using S .

The following property is key to interpreting the partial correlation graph.

Theorem S28. Let $X[\cdot]$ be an n -dimensional, stochastic process satisfying Definition S13. Let \mathcal{G}_X be the corresponding partial correlation graph. Further, let $S \subset [n]$ and $a, b \in [n] \setminus S$, $a \neq b$ such that S separates a from b , i.e. every path from a to b contains at least one node in S . Then

$$a \perp b \mid S.$$

To prove this theorem we need two results which we present first. The proof of Theorem S28 will follow thereafter.

Lemma S29. Let $X[\cdot]$ be an n -dimensional, stochastic process satisfying Definition S13 and let $f = \mathcal{F}\{k_X\}$. Further, define $g(\alpha) := f(\alpha)^{-1}$. Let $A, B \subset [n]$ be disjoint subsets, set $D = [n] \setminus (A \cup B)$, and let $g_{AB}(\alpha)$ be the submatrix obtained by taking rows and columns corresponding to index sets A and B respectively. Then

$$g_{AB}(\cdot) \equiv 0$$

if and only if

$$e_{(A \cup B), D}[\cdot] \text{ is block diagonal, i.e. } e_{(A \cup B), D}[\tau] = \begin{pmatrix} \begin{matrix} \xrightarrow{|A|} & \xrightarrow{|B|} \\ \cdot & \dots & \cdot & 0 & \dots & 0 \\ \vdots & \ddots & \vdots & \vdots & \ddots & \vdots \\ \cdot & \dots & \cdot & 0 & \dots & 0 \end{matrix} \\ \begin{matrix} \xrightarrow{|A|} \\ \xrightarrow{|B|} \\ 0 & \dots & 0 & \cdot & \dots & \cdot \\ \vdots & \ddots & \vdots & \vdots & \ddots & \vdots \\ 0 & \dots & 0 & \cdot & \dots & \cdot \end{matrix} \end{pmatrix}, \quad \forall \tau \in \mathbb{Z}$$

Proof. W.l.o.g. we assume that $A = \{1, \dots, n_A\}$, $B = \{n_A + 1, \dots, n_A + n_B\}$ and $D = \{n_A + n_B + 1, \dots, n\}$. Further, we define $C := \{1, \dots, n_A + n_B\}$, i.e. $C = A \cup B$. Now we fix $\alpha \in [0, 1]$ arbitrary and partition $f(\alpha)$ and $g(\alpha)$ as follows

$$f(\alpha) = \begin{array}{c} \begin{matrix} \text{f}_{CC} \\ \text{C} \left\{ \begin{array}{l} \text{A} \\ \text{B} \end{array} \right. \\ \text{D} \end{matrix} \\ \begin{array}{|c|c|c|} \hline \begin{array}{|c|c|} \hline f_{AA} & f_{AB} \\ \hline f_{BA} & f_{BB} \\ \hline \end{array} & & f_{CD} \\ \hline & f_{DC} & f_{DD} \\ \hline \end{array} \end{array}, \quad g(\alpha) = \begin{array}{c} \begin{matrix} \text{g}_{CC} \\ \text{C} \left\{ \begin{array}{l} \text{A} \\ \text{B} \end{array} \right. \\ \text{D} \end{matrix} \\ \begin{array}{|c|c|c|} \hline \begin{array}{|c|c|} \hline g_{AA} & g_{AB} \\ \hline g_{BA} & g_{BB} \\ \hline \end{array} & & g_{CD} \\ \hline & g_{DC} & g_{DD} \\ \hline \end{array} \end{array}. \quad (27)$$

Further, we define $f^\epsilon = \mathcal{F}\{e_{(A \cup B), D}(\alpha)\}$, which we partition as follows

$$f^\epsilon = \begin{array}{|c|c|} \hline f_{AA}^\epsilon & f_{AB}^\epsilon \\ \hline f_{BA}^\epsilon & f_{BB}^\epsilon \\ \hline \end{array}. \quad (28)$$

We start by applying Theorem S7 with the partition as in (27) to obtain

$$g_{CC} = (f_{CC} - f_{CD}f_{DD}^{-1}f_{DC})^{-1}.$$

We now recognize, using (15), that $g_{CC} = (\mathcal{F}\{e_{C,D}\}(\alpha))^{-1} = (f^\epsilon)^{-1}$. By Corollary S20, $E_{(A \cup B), D}$ satisfies Definition S13 and $\mathcal{F}\{e_{(A \cup B), D}\} = f^\epsilon$ is non-singular $\forall \alpha \in [0, 1]$. From Corollary S14 we then also have that f_{BB}^ϵ is non-singular, and thus we can apply Theorem S7 with the partition in (28) to compute g_{AB} , the upper right sub-matrix of $(f^\epsilon)^{-1}$:

$$g_{AB} = - \left(f_{AA}^\epsilon - f_{AB}^\epsilon (f_{BB}^\epsilon)^{-1} f_{BA}^\epsilon \right)^{-1} f_{AB}^\epsilon (f_{BB}^\epsilon)^{-1}$$

Since the inverses are non-singular, we have $g_{AB} = 0 \Leftrightarrow f_{AB}^\epsilon = 0$. As α was arbitrary this shows

$$g_{AB}(\cdot) \equiv 0 \Leftrightarrow \mathcal{F}\{e_{(A \cup B), D}\}_{AB} \equiv 0 \Leftrightarrow (e_{(A \cup B), D})_{AB} \equiv 0.$$

By Remark S10, this shows that $e_{(A \cup B), D}$ is indeed block diagonal. \square

Lemma S30. Let $X[\cdot]$ be an n -dimensional, stochastic process satisfying Definition S13. Further, let $S \subset [n]$ and $a, b, c \in [n] \setminus S$. Then

$$a \perp b \mid S \cup \{c\} \quad \text{and} \quad a \perp c \mid S \cup \{b\}.$$

imply

$$a \perp b \mid S.$$

Proof. Let $V = S \cup \{a, b, c\}$ and consider the reduced stochastic process $Y = X_V$ with autocovariance sequence $k_Y[\cdot]$, power spectral density $f^Y = \mathcal{F}\{k_Y\}$, and its inverse $g^Y = (f^Y)^{-1}$. We directly observe that $a \perp b \mid S \cup c$ relative to the stochastic process X is equivalent to $a \perp b \mid \{a, b\}^c$ relative to the stochastic process Y , since $V \setminus \{a, b\} = S \cup \{c\}$. Similarly, $a \perp c \mid S \cup \{b\}$ relative to X is equivalent to $a \perp c \mid \{a, c\}^b$ relative to Y . Further, by Corollary S14, f^Y is again full rank, and thus we can apply Lemma S29 with the stochastic process Y twice to obtain

$$g_{ab}^Y \equiv 0 \quad \text{and} \quad g_{ac}^Y \equiv 0.$$

Now define the set $B = \{b, c\}$ and we have $g_{aB}^Y \equiv 0$. We use Lemma S29 in the other direction to get

$$e_{(\{a\} \cup B), S}[\tau] \text{ is block diagonal } \forall \tau \in \mathbb{Z}.$$

Thus, using Corollary S21,

$$e_{\{a, b\}, S}[\tau] \text{ is diagonal } \forall \tau \in \mathbb{Z},$$

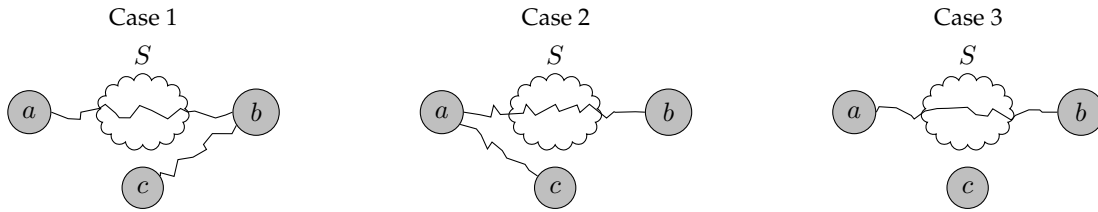
and we have $a \perp b \mid S$ as desired. \square

Proof of Theorem S28. The proof is by backward induction on the number of nodes $k := |S|$ in the set S . For the base case, $k = n - 2$, we have $S = [n] \setminus \{a, b\}$. Hence, S separating a from b simply means that there is no edge between a and b . By Definition S25 this implies $a \perp b \mid S$, as desired.

Now assume that for $k < n - 2$ and all sets $S' \subset [n]$ with $|S'| > k$, that separate a from b we also have $a \perp b \mid S'$.

Next we want to show that the same holds for all such sets with k nodes. To this end, fix $S \subset [n]$, such that $|S| = k$ and S separates a from b . Further, choose an arbitrary node $c \in [n] \setminus (S \cup \{a, b\})$ and observe that $S \cup \{c\}$ separates a from b . Using the inductive assumption this implies $a \perp b \mid S \cup \{c\}$.

Next we consider how a, b and c are connected. Since S separates a and b there are only 3 possibilities, as illustrated below. In particular, there cannot be a path via c from a to b , that does not also go through S .



Case 1 There is a path from b to c that does not go through S . This implies that $S \cup \{b\}$ separates a and c . By the inductive assumption, we therefore have $a \perp c \mid S \cup \{b\}$. Together, with $a \perp b \mid S \cup \{c\}$ Lemma S30 then implies $a \perp b \mid S$ as desired.

Case 2 There is a path from a to c that does not go through S . This implies that $S \cup \{a\}$ separates c from b , and, by the inductive assumption, $c \perp b \mid S \cup \{a\}$. Together, with $a \perp b \mid S \cup \{c\}$ Lemma S30 then implies $a \perp b \mid S$ as desired.

Case 3 There is no path between c and either a or b that does not go through S . We then also have that $S \cup \{b\}$ separates a and c . Therefore, we can treat this case the same as Case 1.

This completes the inductive step and therefore the proof. \square

A.3 A partial correlation graph for stroke recovery data

In this section we describe the implementation we use to estimate the partial correlation graph defined in Section A.2.4 from data.

A.3.1 Estimating the graph from data

Let $N \in \mathbb{N}$ be the number of patients. For each patient $j \in \{1, \dots, N\}$, we are given a time-series $x_j[\cdot]$ with $T_j \in \mathbb{N}$ weekly n -dimensional measurements, i.e. $x_j[t] \in \mathbb{R}^n$ for $t \in \{1, \dots, T_j\}$. This collection $\mathcal{X} := \{x_j[\cdot] | j \in [N]\}$ constitutes our dataset. Since patients overall get better through recovery the $x_j[\cdot]$ sequences generally tend to be increasing. However, we are interested in describing the pattern of recovery, thus we instead investigate the time-series of score improvements from week to week. Further, we subtract the global average of this improvement such that the resulting data has mean zero. More specifically, we define

$$m = \frac{1}{N} \sum_{j=1}^N \left(\frac{1}{T_j - 1} \sum_{t=1}^{T_j-1} x_j[t+1] - x_j[t] \right)$$

and

$$\tilde{x}_j[t] := (x_j[t+1] - x_j[t]) - m \quad \text{for } t \in \{1, \dots, \tilde{T}_j\} \text{ and } j \in \{1, \dots, N\},$$

where $\tilde{T}_j := T_j - 1$ is the length of the processed time-series. Thus, it is reasonable to assume that \tilde{x}_j are samples of a zero-mean WSS process satisfying Definition S13.

Next, we need to estimate the autocovariance sequence of the underlying process. Let $T_{\max} = \max_{j \in [N]} \tilde{T}_j$ and define for $\tau \in -(T_{\max} - 1), \dots, 0, \dots, (T_{\max} - 1)$, the estimate

$$\hat{k}[\tau] := \frac{1}{\#\{j \in [N] | \tilde{T}_j > |\tau|\}} \sum_{j \in [N], \tilde{T}_j > |\tau|} \frac{1}{\tilde{T}_j - |\tau|} \left(\sum_{t=\max\{1, 1-\tau\}}^{\min\{\tilde{T}_j-\tau, \tilde{T}_j\}} \tilde{x}_j[t+\tau] \tilde{x}_j[t]^T \right).$$

Estimates for large values of $|\tau|$ might be noisy which leads to a large variance in the estimated power spectral density⁴³(Chapter 2). Hence, we taper the estimate of the autocovariance sequence using a window function $w[\cdot]$ as follows

$$\tilde{k}[\tau] := w[\tau] \hat{k}[\tau].$$

We choose the *Blackman* window, but note that we also obtained the same graph when using the *Tri-angle*, *Hann*, or *Hamming* windows.

Next, we apply the fast Fourier transform to get samples of $f(\alpha) = \mathcal{F}\{\tilde{k}\}(\alpha)$, at the values $\alpha \in \left\{ \frac{0}{2T_{\max}-1}, \frac{1}{2T_{\max}-1}, \dots, \frac{2(T_{\max}-1)}{2T_{\max}-1} \right\}$. We then compute $d(\alpha)$ defined in (25) for these values. Next, we need to identify entries a, b in this matrix-valued sequence such that $d_{a,b}(\cdot) \equiv 0$. To this end we compute $\|d_{a,b}(\cdot)\|_{\ell^1}$ and sort the values obtained in this way. Figure I shows the values associated with each edge in descending order. We identify a drop after the 6th edge, and thus visualize the six dominant edges in Figure II.

A.3.2 Reliability of the algorithm

Finally, we estimate the reliability of our procedure using Bootstrapping⁴⁴. Specifically, we randomly draw with replacement N time-series from \mathcal{X} to produce a bootstrap replicate dataset \mathcal{X}' . Then we apply the procedure from Section A.3.1 to obtain a new graph with 6 edges. This we repeat 10'000 times and count how often a particular edge is missing, respectively how often a particular new edge occurs. Table ?? shows the obtained frequencies.

A.3.3 Partial correlation graphs for left and right supratentorial strokes

We repeat the procedure from Section A.3.1 separately for the groups of patients that suffered a left or right supratentorial stroke. In Figure III we visualize the top six edges obtained in this way for each group.

Table S1: Definitions of the investigated domains of the Activities and Participation component according to the International Classification of Functioning, Disability and Health.

ICF domain	Definition
Interpersonal interactions and relationships	This domain is about carrying out the actions and tasks required for basic and complex interactions with people (strangers, friends, relatives, family members and lovers) in a contextually and socially appropriate manner.
Mobility	This domain is about moving by changing body position or location or by transferring from one place to another, by carrying, moving or manipulating objects, by walking, running or climbing, and by using various forms of transportation.
Self-care	This domain is about caring for oneself, washing and drying oneself, caring for one's body and body parts, dressing, eating and drinking, and looking after one's health.
Communication	This domain is about general and specific features of communicating by language, signs and symbols, including receiving and producing messages, carrying on conversations, and using communication devices and techniques.
Learning and applying knowledge	This domain is about learning, applying the knowledge that is learned, thinking, solving problems, and making decisions.
General tasks and demands	This domain is about general aspects of carrying out single or multiple tasks, organizing routines and handling stress. These items can be used in conjunction with more specific tasks or actions to identify the underlying features of the execution of tasks under different circumstances.
Domestic life	This domain is about carrying out domestic and everyday actions and tasks. Areas of domestic life include acquiring a place to live, food, clothing and other necessities, household cleaning and repairing, caring for personal and other household objects, and assisting others.

Reference: World Health Organization. Towards a common language for functioning, disability and health: ICF. Geneva, 2002.

Table S2: Scoring of the items of the Lucerne ICF-based Multidisciplinary Observation Scale (LIMOS).

Score	Description
1	the patient is not able to fulfil a task at all or needs more than 75% of assistance (i.e., complete assistance)
2	the patient is able to fulfil a task with an assistance of 25–75% (i.e., severe assistance)
3	the patient is able to fulfil a task with an assistance of <25%, or under supervision (i.e., moderate assistance)
4	the patient is able to fulfil a task independently, but needs increased time and/or auxiliary materials/ aids (i.e., slight assistance)
5	the patient is able to fulfil a task independently (i.e., no assistance needed)

Table S3: Fraction of bootstrap samples in which an edge was missing or an additional edge was found.

	Missing edges (%)	Extra edges (%)
Interpersonal interactions and relationships Self-care	24.21	
General tasks and demands Learning and applying knowledge	1.98	
Mobility Self-care	1.19	
General tasks and demands Self-care	1.02	
Domestic life General tasks and demands	0.00	
Domestic life Learning and applying knowledge	0.00	
Domestic life Mobility		15.18
Communication Self-care		6.40
Communication Interpersonal interactions and relationships		3.52
Communication Learning and applying knowledge		1.78
Learning and applying knowledge Self-care		0.77
Communication Domestic life		0.32
Interpersonal interactions and relationships Learning and applying knowledge		0.16
General tasks and demands Mobility		0.13
Interpersonal interactions and relationships Mobility		0.08
Domestic life Self-care		0.04
General tasks and demands Interpersonal interactions and relationships		0.02
Communication General tasks and demands		0.00
Communication Mobility		0.00
Domestic life Interpersonal interactions and relationships		0.00
Learning and applying knowledge Mobility		0.00

Figure S1. For each pair a, b of nodes we visualize the ℓ^1 -norm of the corresponding entry in $d(\cdot)$ as computed in (25). We identify a drop after the 6th edge (red line) and thus retain only the first six edges.

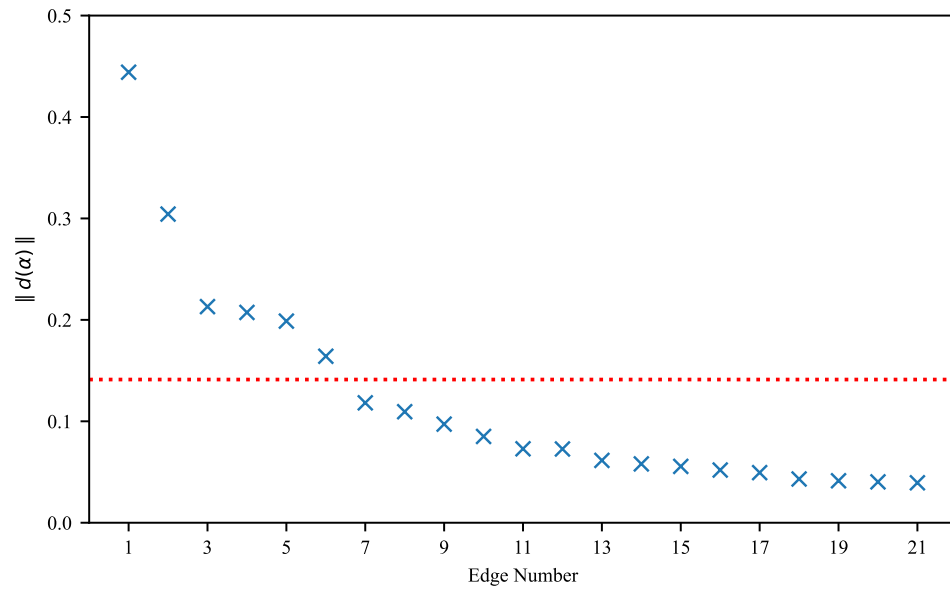


Figure S2. Partial correlation graph that visualizes the six dominant edges identified in Figure S1. The thickness of an edge between nodes a and b is proportional to $\|d_{ab}\|_{\ell^1}$ as defined in (26).

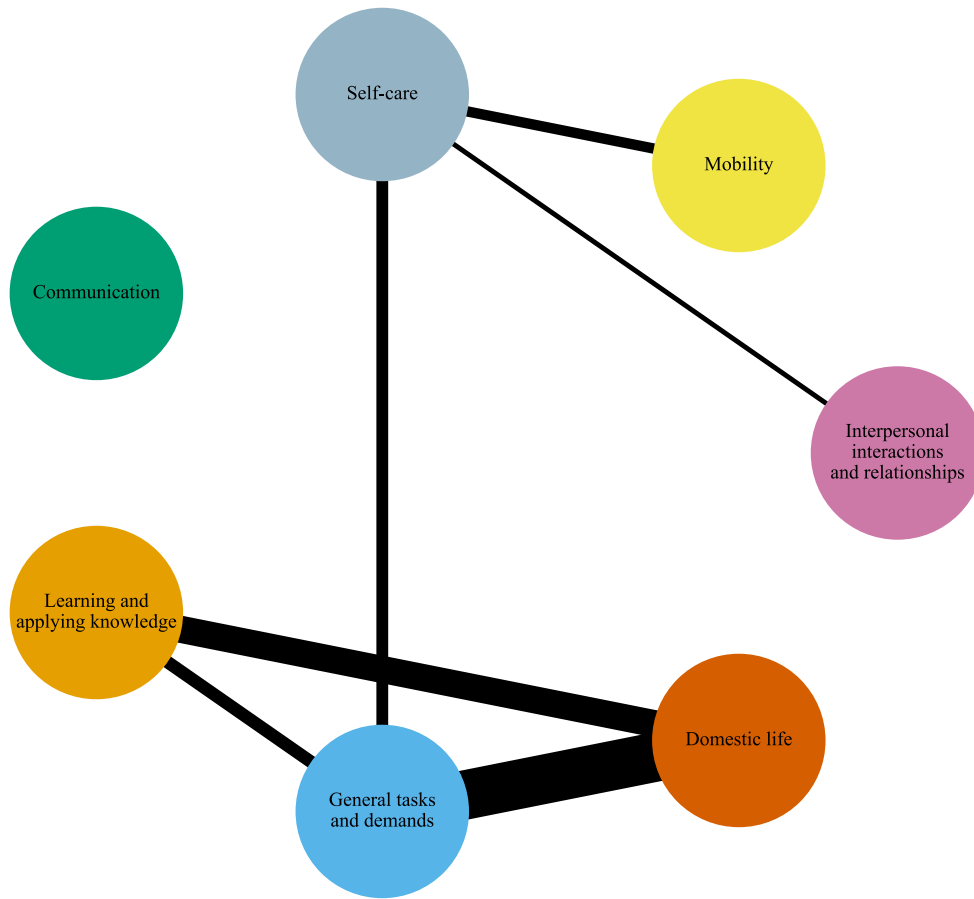


Figure S3. We repeat the analysis from Section A.3.1 separately for patients that suffered a left or right supratentorial stroke and visualize the top 6 edges in each case.

